EXTRUSION BASED CERAMIC 3D PRINTING - PRINTER DEVELOPMENT, PART CHARACTERIZATION, AND MODEL-BASED SYSTEMS ENGINEERING ANALYSIS

by

Piyush Shrihari Pai Raikar

A Thesis

Submitted to the Faculty of Purdue University

In Partial Fulfillment of the Requirements for the degree of

Master of Science in Mechanical Engineering

Department of Mechanical and Energy Engineering at IUPUI

Indianapolis, Indiana

December 2020

THE PURDUE UNIVERSITY GRADUATE SCHOOL
STATEMENT OF COMMITTEE APPROVAL

Dr. Jing Zhang, Chair

Department of Mechanical and Energy Engineering

Dr. Mangilal Agarwal

Department of Mechanical and Energy Engineering

Dr. Babak Anasori

Department of Mechanical and Energy Engineering

Approved by:

Dr. Jie Chen

Head of the Graduate Program

Dedicated to my grandparents Sulochana and Venkatesh;

Ratan and Narendra;

My parents Madhura and Shrihari;

And my Bhai.

ACKNOWLEDGMENTS

Sincerely grateful to Dr. Jing Zhang for his valuable guidance and mentorship through the course of my M.S. program. I really appreciate his support and help with providing all the resources and the knowledge base for the completion of this thesis project. I would also like to thank Dr. Mangilal Agarwal and Dr. Babak Anasori for being on my thesis committee and for all the inputs that made me understand my work better and look at the research domain from a different perspective. Thank you for your time and consideration.

This research was partially supported by the "Human Resources Program in Energy Technology" of the Korea Institute of Energy Technology Evaluation and Planning (KETEP), granted financial resources from the Ministry of Trade, Industry & Energy, Republic of Korea. (No. 20194030202450) and by the National Research Foundation of Korea (NRF) grant funded by the Korea government (MSIP) (2018R1A5A6075959).

I would also like to thanks my lab mates Tejes, Nishant, Harshal, Abhilash, Swapnil, Anvesh, Xuehui, Lingbin and Jian for their continued support throughout my thesis project. Lastly, my friends Kalpak, Prasad, Rajat, Abhishek, Pental, Simran and my brother Dr. Vipul for always believing in me and for your support and motivation.

TABLE OF CONTENTS

LIST OF TABLES

LIST OF FIGURES

ABSTRACT

Ceramics have been extensively used in aerospace, automotive, medical, and energy industries due to their unique combination of mechanical, thermal, and chemical properties. The objective of this thesis is to develop an extrusion based ceramic 3D printing process to digitally produce a casting mold. To achieve the objective, an in-house designed ceramic 3D printer was developed by converting a filament based plastic 3D printer. For mold making applications, zircon was selected because it is an ultra-high temperature ceramic with high toughness and good refractory properties. Additionally, alumina, bioglass, and zirconia slurries were formulated and used as the feedstock material for the ceramic 3D printer.

The developed 3D printing system was used to demonstrate successful printing of special feature parts such as thin-walled high aspect ratio structures and biomimetically inspired complex structures. Also, proof of concept with regard to the application of 3D printing for producing zircon molds and casting of metal parts was also successfully demonstrated.

To characterize the printed parts, microhardness test, scanning electron microscopy (SEM), and X-ray diffraction (XRD) analyses were conducted. The zircon samples showed an increase in hardness value with an initial increase in heat treatment temperature followed by a drop due to the development of porosity in the microstructure, caused by the decomposition of the binder. The peak hardness value for zircon was observed to be 101±10 HV0.2. Similarly, the microhardness values of the other 3D printed ceramic specimens were observed to increase from 37±3 to 112±5 HV0.2 for alumina, 23±5 to 35±1 HV0.2 for bioglass, and 22±5 to 31±3 HV0.2 for zirconia, before and after the heat-treatment process, respectively.

Finally, a system model for the ceramic 3D printing system was developed through the application of the model-based systems engineering (MBSE) approach using the MagicGrid framework. Through the system engineering effort, a logical level solution architecture was modeled, which captured the different system requirements, the system behaviors, and the system functionalities. Also, a traceability matrix for the system from a very abstract logical level to the definition of physical requirements for the subsystems was demonstrated.

1. INTRODUCTION

1.1 Literature Review

1.1.1 Additive Manufacturing of Ceramics

Additive manufacturing or 3D printing is one of the most innovative and fastest-growing technologies in the manufacturing domain. Through the use of 3D printing methods it is possible to develop a wide variety of complex shapes in a relatively shortened time frame and at lower costs. The incorporation of 3D printing in industry has drastically changed the product development process. The academic and research fields have immensely benefited from this technology. With the capabilities of using different compatible materials like metals, plastics, ceramics, and even human tissue the application of 3D printing are limitless. As a part of this study, we will be focusing on Zircon, which is a ceramic material with efforts towards developing a simple and viable process to develop zircon as a potential 3D printing material and contribute towards the advancements of this vast field of additive manufacturing.

Ceramics as a result of their excellent properties in terms of strength and hardness, thermal and chemical stability, and also good optical, electrical and magnetic performance are used in a wide variety of applications and have found its way into different industries such as chemical, mechanical, electronics, aerospace and biomedical engineering[1]. In order to make the best of the benefits provided from the use of ceramics, the additive manufacturing domain has also progressed and developed different 3D printing technologies that can efficiently make use of ceramics. Based on the type and form of the feedstock used for printing, ceramic 3D printing can be classified into slurry-based, powder-based and bulk solid-based printing processes[1]. The different types of ceramic 3D printing processes are list in Table 1.1

The slurry-based ceramic 3D printing process consists of feedstock containing fine ceramic particles as liquid or semi-liquid systems. Based on the solid loading and viscosity of the system the feedstock can be either in the form of an ink or paste. This slurry-based feedstock can be 3D printed in two ways, by photopolymerization process using technologies such as SL, DLP and TPP or by an extrusion process using technologies like IJP or DIW. The basic working principle of

technologies like SL, DLP and TPP is to selectively cure a liquid surface consisting of a photocurable medium and ceramic particles through exposure to a light source having particular specifications and method of exposure for each type of process[2][3][4]. Similarly, the basic working principle of technologies like IJK and DIW is to extrude a paste-like feedstock of a certain viscosity which contains ceramic particles and other additives like a binder through a nozzle either in a continuous or a drop-on-demand (DOD) manner so as to form the desired shape in a layer by layer fashion[5].

Table 1.1: Ceramic 3D printing technologies[1]

Feedstock Form	**3D printing technology**	**Abbreviation**
Slurry-based	Stereolithography	SL
	Digital light processing	DLP
	Two-photon polymerization	TPP
	Inkjet printing	IJP
	Direct ink writing	DIW
Powder-Based	Three-dimensional printing	3DP
	Selective laser sintering	SLS
	Selective laser melting	SLM
Bulk solid-based	Laminated object manufacturing	LOM
	Fused deposition modelling	FDM

The powder-based ceramic 3D printing process consists of feedstock in the form of a powdered bed contacting of loose ceramic particles. In this process, the parts are formed by bonding the ceramic particles either by using a liquid binder or by fusion of the particles utilizing the thermal energy from a laser beam to form the desired shapes. In the 3DP process, an organic liquid binder is deposited on the powder bed which acts like a glue and solidifies to bond the particles to form a layer as per the designed shape[6]. The SLS and SLM technologies work on the principle of using a laser beam to generate enough thermal energy so as to cause the fusion of the particles thereby forming the designed shape[7]. The difference between the SLS and the SLM technologies is that due to the refractory properties and high melting temperatures of ceramics in the SLS process, a secondary binder material is used to lower the target melting points thereby allowing for the fusion of the particles due to the melting of the binder material, requiring a lower energy input as compared to the SLM process where enough energy is generated from the source to melt the ceramic particle.

The bulk solid- based ceramic 3D printing process consists of two main technologies namely, LOM and FDM. In the LOM process, the feedstock in the form of a thin sheet of material is prepared and cut as per the cross-section of the sliced digital CAD model using lasers to form a layer[8]. A subsequent layer is formed on top of the previous layer and the two layers are bonded by applying an adhesive, heat and mechanical compression. Similarly, in the FDM process, the feedstock in the form of a continuous filament is heated and extruded through a moving nozzle which then deposits the material on a print bed to form a layer of the designed part[9]. The print bed than further relocates to form the subsequent layers of the 3D part.

1.1.2 Zirconium Silicate (ZrSiO4)

Zirconium Silicate, commonly known as Zircon is a natural mineral belonging to the neosilicate group. It has a tetragonal crystal structure as shown in Figure 1.1. Zircon exclusively develops through early liquid magmatic crystallization in alebite-bearing acidic rocks such as granites, diorites, syneties, and their pegmatites[10]. The majority of Zircon available is obtained from heavy-mineral sand mining[11]. This is achieved in three main steps: mining, wet concentration and dry separation[12]. The end product of these processes is Zirconium Silicate which is commercialized in sand and milled form with specifications varying based on the application.

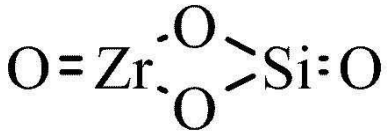

Figure 1.1Crystal Structure of Zircon (ZrSiO4)

Zirconium Silicate (ZrSiO4) is a very hard, highly refractive, birefringent and refractory material[11]. The properties that make zircon a good refractory material are, it has a very high melting point temperature: > 2430°C[11]. The zircon sands have a fire-resistance equal to pyrometric cone 39/40. Below a temperature of 1673°C [13] Zircon remains stable, but it can be dissociated[14] into Zirconia (ZrO2) and Silicone dioxide (SiO2) if exposed to greater temperatures and can be recombined under slow cooling. It has very low and regular thermal

expansion, poor wettability by molten metals, excellent thermal conductivity, and chemical stability. Because of the above-mentioned refractory properties and the characteristics like low acidity, its ability to bind easily with all organic and inorganic sand binders, and its ability to form fine grains make zircon a very useful and convenient material for use as a molding base material in the casting industry. The properties that make zircon a suitable material for mold applications are shown in Table 1.2

Table 1.2: Material Properties of Zircon[11]

Properties	**Zircon**
MOHS hardness	7 - 7 ½
Bulk density dry (kg/m3)	2,563-2,964
Apparent density (g/cm3)	4.4-4.7
Grain shape	angular/ round
Thermal expansion (mm/o K)	0.003
Melting point (o C)	2,038-2,204

1.2 Motivation and Objective

In recent years, there has been a drastic change in the manufacturing landscape due to the advancements of additive manufacturing technologies. Due to the development of different 3D printing technologies and material compatibilities, it is now possible to utilize this process in applications from the production of a small-scale prototype parts to the production of large quantity finished products. However, the widespread utilization of ceramic materials through the 3D printing process other than in pottery applications is currently limited to a small scale and limited number of domains such as bio-engineering and electronics, mostly due to the nature of the ceramic materials and limited access to technologies capable of using it efficiently.

Through this work, we aim to utilize Zircon a common and abundantly available ceramic material to make it compatible with 3D printing so that we can make use of all the desirable

properties of this material for printing parts for various applications including printing of molds. Along with this, we also want to develop a 3D printing methodology that is cost-efficient, simple and easily accessible to anyone that requires and finds an application for this material.

2. DEVELOPMENT OF CERAMIC 3D PRINTER

2.1 Introduction

Based on the literature study, we can see that there are different types of additive manufacturing methods and processes available for ceramic 3D printing. These technologies are based on principles such as photopolymerization, extrusion, laser sinter, and fused deposition. However, due to the material's inherent properties such as high melting temperature, high strength, etc. there are many challenges related to the efficient fabrication of ceramics through the use of 3D printing technologies. Further analysis also suggests that along with choosing the right type of 3D printing process based on the desired application, the formulation and composition of the feedstock is a very important factor in determining the properties of the final product. Although studies have shown that ceramic 3D printing processes like IJP, SLS, etc. are capable of producing fine quality parts, these processes are very time consuming and not cost and energy-efficient. In addition, materials like zircon, which have a very high melting temperature, are not suitable to be formulated into an ideal feedstock for such processes.

To overcome some of the above-mentioned difficulties, we have developed a customized desktop printer that uses a slurry-based feedstock and works on the principles of freeform fabrication technique to 3D print ceramic parts[15]. The printer is equipped with an extrusion mechanism which extrudes the zircon slurry through a movable nozzle and deposits material on the print bed as per the cross-section of the designed part one layer at a time. The developed machine has a very simple working mechanism and is very cost-effective to setup.

2.2 Customized 3D Printer

In order to develop an extrusion-based customized 3D printer, a plastic fused deposition modeling 3D printer similar to a printer as shown in Figure 2.1, is used for the base architecture. This type of 3D printer framework is chosen as it has a very simple and stable design and is easily available as a DIY kit at a reasonable price.

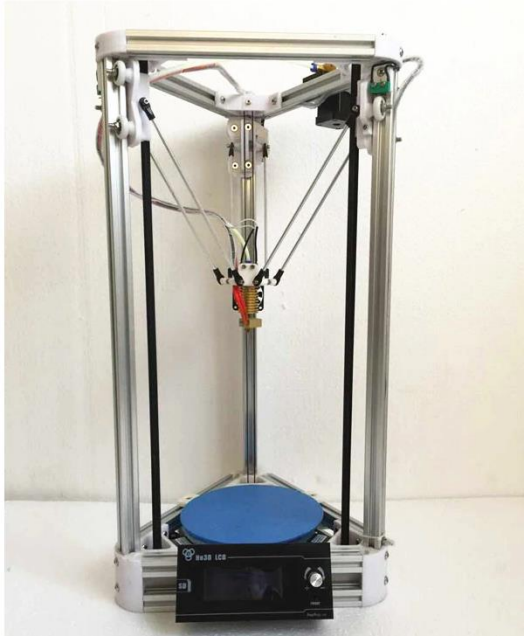

Figure 2.1: KOSSEL ROSTOCK RepRap Delta 3D Printer DIY Kit DLT -180

The customized ceramic 3D printer as shown in Figure 2.2, is built on an aluminum frame and has a height of 600 mm and a width of 320 mm. There is a stepper motor mounted at the base of each of the three aluminum structural beams that are responsible for the motion of the extruder along the three-axis. These motors have a phase voltage of 2.55 V, a phase current of 1.7 A, and a torque of 2.2 N-cm. To facilitate this motion, these stepper motors are connected to a slider mounted on the vertical beam via a pulley system. These sliders are also connected to the extruder arms through which the motion is transmitted to the extruder. At the top of each vertical beam, there is an end-stop switch that constraints the vertical motion and acts as a co-ordinate point for homing the printer. The setup for these motors is shown in Figure 2.3.

To facilitate the use of ceramic slurry as the feedstock, the primary modification required was in the form of a stand-alone extrusion system capable of feeding the highly loaded ceramic slurry through the nozzle while printing. To do so a special mount that can accommodate the extruder system is designed and attached to the extruder arms, as shown in Figure 2.4 (a). The extruder system consists of a cartridge that holds a syringe of 30 ml volume in which the slurry is loaded and a bipolar stepper motor with a linear actuator that pushes on the plunger of the syringe thereby extruding the zircon slurry during the printing process. The syringe used has a leur-lock

tip to which nozzles of different sizes can be attached. Figure 2.4 shows the different parts of the extruder system assembly. The bipolar extrusion stepper motor used is Ametek 57F4A-3.25-099, which has a phase voltage of 3.25 V, a phase current of 2A, and a maximum thrust force of 200 lb.

Figure 2.2: Customized Ceramic 3D Printer

(a)

(b)

Figure 2.3: Stepper Motor Setup for Controlling the Position of the Extruder: (a) Stepper Motor Mounted at the Base and Attached Via Belt and Pulley, (b) Slider Mounted on the Vertical Beam with End-Stop Switch at the Top End

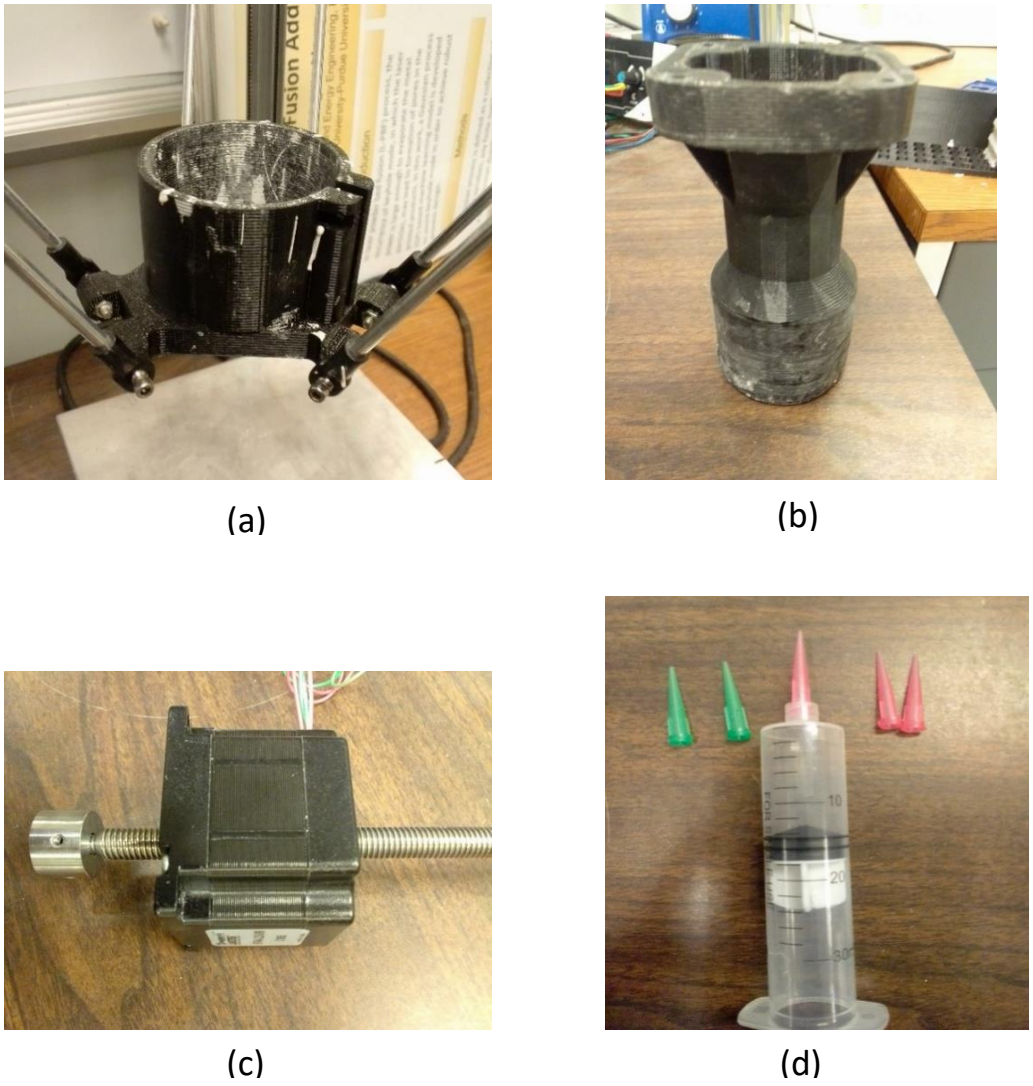

Figure 2.4: Different Parts of the Extrusion System: (a) Custom Mount (b) Custom Cartridge to Hold the Loaded Syringe, (c) Bipolar Stepper Motor with Linear Actuator, (d) 30 ml Leur-Lock Tip Syringe with Plunger and Nozzles

The primary control for the printer i.e. signals to the positional stepper motors, the extrusion stepper motor and the thermistor is programmed using Marlin firmware and execute through the user interface of 3D printing software Repetier Host (Hot-World GmbH & Co. KG). The hardware setup of the control system includes an Arduino Mega 2560 microcontroller on top of which the RAMPS v1.4 controller board is attached as can be seen in Figure 2.5. The microcontroller consists of three A4998 series stepper motor drivers to which the three positional stepper motors are connected. Apart from this, there is also a thermistor, which is a remnant from

the plastic fused deposition printer extrusion system, the output of which is used as a trigger signal to initiate the ceramic extrusion printing process. The extrusion stepper motor is controlled using a stepper motor driver (TB67S249-FTG series), which is set up on a separate breadboard and power by an external 48 V power supply. However, it still receives its operational signals via the Arduino microcontroller through the Marlin. Figure 2.6 shows the extrusion motor controller setup.

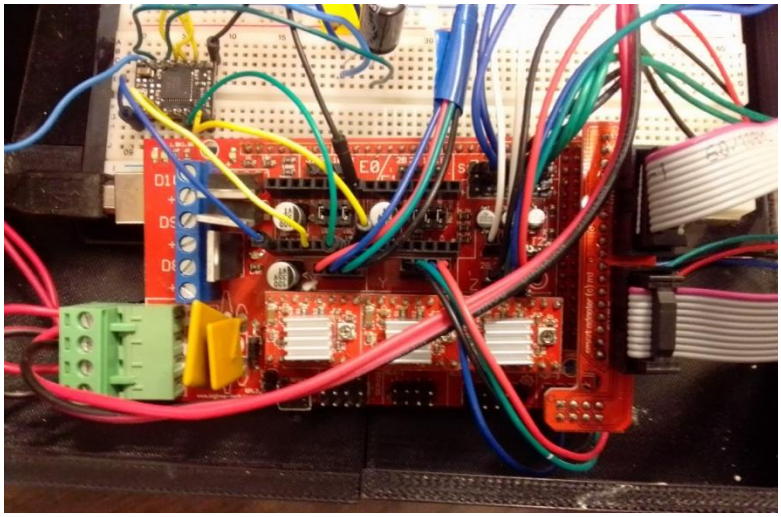

Figure 2.6: Arduino Mega 2560 with RAMPS v.14 Microcontroller

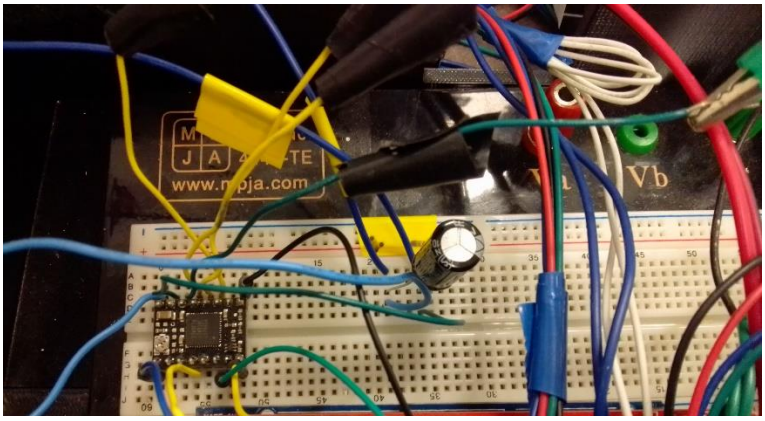

Figure 2.5: Stepper Motor Driver Setup for Extrusion Motor

3. CERAMIC SLURRY FORMULATION

3.1 Slurry Formulation Process

3.1.1 Zircon Slurry Material Composition

To use the extrusion process for 3D printing, a highly loaded[16] paste-like slurry of ceramic of appropriate dynamic viscosity was prepared. The slurry consists of four components, Zirconium Silicate (Zircon) powder as the base slurry material, Polyvinyl pyrrolidone (PVP) as the binder, Darvan as the deflocculant and DI water as the base mixing media. Through multiple iterations of using different material composition, the slurry composition was modified and adjusted to achieve a viscosity suitable to be extruded using the extrusion mechanism incorporated in the customized 3D printer.

The Zircon powder, ZR-720 (Atlantic Equipment Engineers) with chemical formula ZrSiO4 and molecular weight 183.31 g/mol is used as the base material for the slurry formulation. The mechanical properties of the final slurry composition are majorly driven by the properties of this base material and accounts for about ~60 vol% of the total slurry volume. The properties of the Zircon powder as obtained from the manufacturer are shown in Table 3.1

Table 3.1: Material Properties of ZR-720 Powder (zircon)

Properties	**Values**
Melting Point	2550 °C
Density	4.56 g/cm^3
Particle Size	0.7 – 1.0 Micron
Purity	99.9 %
Form	Powder

The base slurry material, Zircon powder is an argillaceous material. When this fine powder is dispersed in the aqueous mixing media DI water, due to the positive electrical charges between the particles, they are attracted to one another and form three-dimensional structures that lead to the formation of clumps resulting in a non-homogeneous mixture. This phenomenon which causes agglomeration of the aqueous mixture is known as flocculation[17] and it adversely affects the

viscosity and thus the flowability of the slurry. To overcome the effects of flocculation Darvan® 821A (R.T. Vanderbilt Company, Inc., Norwalk, CT) is added to the mixture. Darvan® 821A is a water-soluble solution of ammonium polyacrylate. It has a molecular weight of 3500 g/mol, a density of 1.25 mg/m3 and a very low ash content[18][19]. Its molecules are negatively charged[20] and attach to the Zircon particles and cause them to repel and thus remain suspended in the aqueous mixture. The active agent in Darvan is polyacrylic acid. The total ceramic slurry volume consists of about ~2.8 vol% of Darvan® 821A as the deflocculating agent. The chemical structure of Darvan® 821A is shown in Figure 3.1

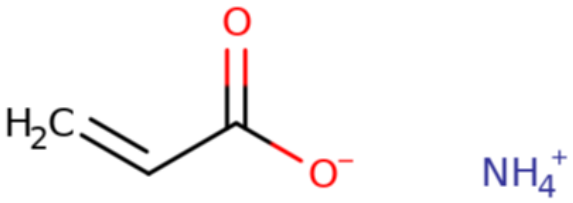

Figure 3.1: Chemical Structure of Darvan® 821A
(Ammonium Polyacrylate)

Polyvinyl pyrrolidone (PVP, 1-Ethenyl-2-pyrrolidinone homopolymer, Sigma- Aldrich, St. Louis, MO) with linear formula (C6H9NO)n and average molecular weight ~ 55,000 g/mol, which is a water-soluble polymer is used as a binder in the slurry formulation. It acts as a rheological modifier[20] thereby affecting the viscosity of the final slurry composition. It increases the yield point of the slurry, allow for a controlled flow, and shape retention during extrusion and post extrusion respectively[21][22]. To achieve a slurry viscosity suitable for extrusion the amount of PVP used needs to be controlled, and it makes up about ~4.1 vol% of the total relative volume of the slurry. PVP has a melting point of 150 C and its density is 1.2 g/cm3 and is available as a liquid. The chemical structure of PVP is shown in Figure 3.2

The remainder of the volume of the slurry is made up of DI water, which acts as the base mixing media to formulate the ceramic slurry. The volume of DI water added needs to be controlled to a specific level such that there is enough mixing media to allow all the components of the slurry to mix well and have good flowability when extruded. However, the volume of DI

water cannot be excessive as higher water content can lead to higher shrinkage rates in the 3D printed parts if any post-processing heat-treatment is performed, thereby affecting the dimensional properties of the printed specimen. In this study, we use about ~32.8 vol% of DI water relative to the total volume of the slurry. The detailed procedure for slurry formulation is described in the next section.

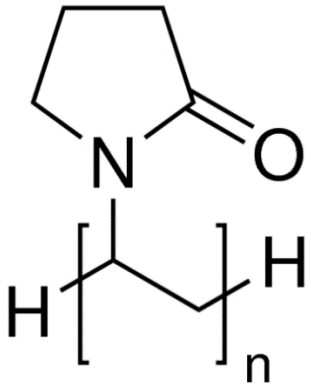

Figure 3.2: Chemical Structure of Polyvinyl Pyrrolidone (PVP)

3.1.2 Zircon Slurry Formulation Procedure

For zircon to be used as a material for the customized 3D printer, a slurry-based feedstock is developed. Based on the concepts used for Alumina (Al2O3) CeraSGels preparation, studied by researcher Dr. Valerie Lynn Wiesner related to her work on injection molding of aqueous ceramic suspension gels[20] , an aqueous slurry of zircon powder containing a binder, a deflocculation agent and DI water is prepared. Table 3.2 lists the different components of the ceramic slurry.

Table 3.2: Component Composition of Zircon Slurry Feedstock

Slurry Component	Form	Component Function
Zirconium Silicate	Powder	Base slurry material
Polyvinyl pyrrolidone (PVP)	Powder	Acts as the binder in the slurry
Darvan® 821A	Liquid	Acts as the deflocculant in ceramic slurry
DI Water	Liquid	Base mixing media

A homogeneous mixture of all the components is obtained by ball milling using a Fritsch planetary ball mill PULVERISETTE 6 model, shown in Figure 3.3. We have chosen ball milling as a mixing process to cause the transformation in the slurries rheological behavior. It changes the slurry behavior from shear thickening to shear thinning depending on the milling/mixing time[23]. This shear thinning nature of the slurry allows for improved processibility while extrusion. I our study we observed that a minimum of 10 hours of mixing in the ball mill is required to obtain a homogeneous slurry, with appropriate viscosity to be used as a feedstock material for the 3D printing application. The detailed slurry formulation process is described further in this section.

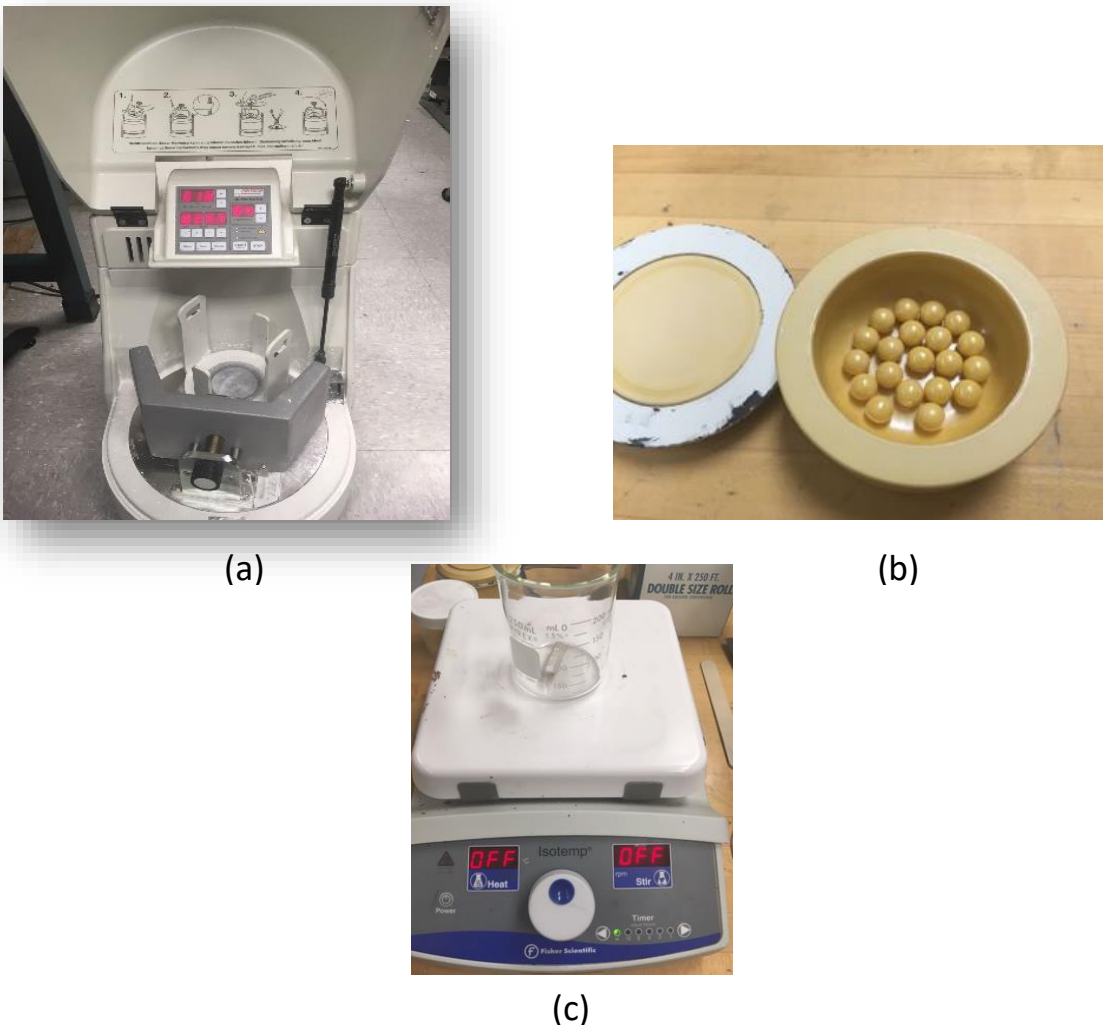

Figure 3.3: (a) Fritsch PULVERISETTE 6 - Planetary Ball Mill (b) Zirconia (ZrO2) Ball Mill Jar and Milling Media (c) Magnetic Stirrer Setup Used for Binder Mixture

At the beginning of the slurry formulation process, the quantities of all the slurry components are carefully measured. The quantity of both solid and liquid components is measured in terms of mass in grams (gm) using a sensitive digital weigh scale. The slurry formulation process is divided into three stages. Stage 1 includes preparation of the polymer binder and DI water mixture; Stage 2 includes preparation of the mixture of Zircon powder, the deflocculant, and DI water; and Stage 3 includes the addition of the binder mixture to the ceramic mixture. The ball mill jar and the milling media used in this process is made of Zirconium Oxide (ZrO2) and has a volume of 80 ml as shown in Figure 3.3 (b).

The details regarding each stage of the slurry formulation process is as follows:

- Stage 1: Mixture of Polyvinyl pyrrolidone (PVP) and DI Water
    - Measured quantities of Polyvinyl pyrrolidone (PVP) and DI water are added to a beaker and set up on a magnetic stirrer for mixing shown in Figure 3.3 (c)
    - The magnetic stirrer is set up at 350 RPM and the mixing process is carried out for approximately 150 minutes to allow the PVP powder to dissolve completely.
    - The mixing beaker is covered with plastic wrap to avoid any spillage.
- Stage 2: Mixture of Zircon, Darvan® 821A, and DI Water
    - The total quantity of zircon powder to be added to the slurry is divided into 5 parts.
    - Measured quantity of one part of zircon powder along with total quantities of Darvan® 821A and DI Water is added to the ball mill jar.
    - The ball mill machine is set up to rotate constantly at 310 RPM.
    - After every interval of 30 minutes, each partly quantity of zircon powder is further added to this mixture for a total of 3 additions.
- Stage 3: Addition of PVP – DI Water mixture to the ball mill
    - 30 minutes after the 3rd addition of zircon powder, the PVP – DI Water mixture from the magnetic stirrer is added to the ball mill machine along with the final addition of the zircon powder.
    - After the addition of all the slurry components, the mixture is kept in the ball mill for a minimum of 10 hours with constant rotation at a speed of 310 RPM.

For convenience, Stage 1 and Stage 2 of the process is carried out simultaneously, so that the binder-DI water mixture is available to be added to the ball mill along with the final Zircon powder addition for the final stage. After letting the mixture run in the ball mill for at least 10 hours, a homogenous mixture of highly loaded slurry of Zircon is obtained. This slurry can be directly loaded into the extrusion syringe of the 3D printer and be used for printing parts. The leftover slurry can be left running in the ball mill and can be used at a later time. The ball mill needs to be kept running to keep the slurry in homogenous form and to avoid the agglomeration of the zircon and binder and separation of the dispersant. The final slurry as obtained from the ball mill machine is shown in Figure 3.5

Figure 3.4: Zircon Slurry Retrieved from the Ball Mill

In this study, to obtain a slurry composition with viscosity that is appropriate for extrusion using the 3D printer, multiple batches with the same total mass but with different combinations of component compositions are prepared. Each batch of the slurry is then tested for its usability by performing test print. The results of this experiment to obtain the ideal slurry composition is presented in the next chapter. One thing to be noted is that due to variations in quantities measured for each component, it is not possible to obtain multiple batches of slurry with identical properties. However, Table 3.3 lists the vol% composition for each slurry component that provides the best printing results and can be referenced as the ideal composition for the preparation of the Zircon slurry feedstock.

Table 3.3: Zircon Slurry Composition for 3D Printer Feedstock

Slurry Component	**Volume percentage (vol%)**
Zirconium Silicate	86.907
Polyvinyl pyrrolidone (PVP)	1.63
Darvan® 821A	1.04
DI Water	10.41

3.1.3 Ceramic Slurry Formulation for Alumina, Bioglass, and Zirconia

Once a stable slurry formulation process was established for formulating a highly loaded aqueous slurry of zircon, the same methodology was used to formulate slurries of alumina, bioglass and zirconia. Apart from the change in the base ceramic material, the slurry consists of same material for binder and deflocculant as used for the Zircon slurry i.e. PVP and Darvan® 821A respectively, and with DI water acting as the base mixing media. For the alumina slurry, A-16 SG Alumina (particle size d50 is 0.5 µm, Almatis GmbH, Ludwigshafen, Germany) is used as the base material. Similarly for bioglass and zirconia slurries, Bioglass 45S5 powder (d50 53 □m, Mo-Sci Corporation, Rolla, MO, USA) and Zirconia powder (d50 44 □m, Accumet Materials Co, Ossining, NY, USA) respectively, are used as the base ceramic materials. The content for each of the slurry with respect to the volume compositions of the base material, the binder, the deflocculant and the mixing media is modified accordingly to obtain a quality of slurry with appropriate viscosity to be compatible with the developed 3D printing system. The different material compositions used for the slurry formulation are listed in Tables 3.4 –Table 3.6

Table 3.4 lists the vol% composition for each component used in the formulation of alumina slurry. Similarly, vol% compositions for bioglass and zirconia slurries are shown in Table 3.5 and Table 3.6 respectively.

Table 3.4: Alumina Slurry Composition for 3D Printer Feedstock[15]

Slurry Component	**Volume percentage (vol%)**
Alumina	54.9
Polyvinyl pyrrolidone (PVP)	2.5
Darvan® 821A	4.2
DI Water	38.4

Table 3.5: Bioglass Slurry Composition for 3D Printer Feedstock[15]

Slurry Component	Volume percentage (vol%)
Bioglass	49.78
Polyvinyl pyrrolidone (PVP)	5.14
Darvan® 821A	3.92
DI Water	41.15

Table 3.6: Zirconia Slurry Composition for 3D Printer Feedstock[15]

Slurry Component	Volume percentage (vol%)
Zirconia	55.16
Polyvinyl pyrrolidone (PVP)	4.14
Darvan® 821A	3.92
DI Water	36.77

4. 3D PRINTING AND CHARACTERIZATION OF CERAMIC SPECIMEN

4.1 Model and 3D Printer Setup

To operate the customized 3D printer, an open-source software Repetier Host is used. It provides a simple user interface that can be used to set up the part model and control the 3D printer. It also has a built-in slicer function that is used to generate the G-Code based on the STL model of the part that is uploaded. It communicates the signals and commands to the printer via Marlin firmware which is flashed onto the Arduino microcontroller that is used for the printer. Before the 3D printer can be used, the software has to be configured such that the customized printer is compatible. One of the important parameter that is required to be set up is the physical dimensions. After implementing all the modification to make it compatible for extrusion of ceramic slurry, the new dimensions for printable radius and height is 67.5 mm and 222.5 mm respectively.

Table 4.1: Printing Parameters for Print Quality Control

Printing Parameter	Value (optimum/suggested)	Effect
Nozzle Diameter	0.5 mm	Needs to be controlled to obtain ideal layer thickness
Bed Temperature	70 °C	Needs to be controlled to obtain stable layering
Extrusion Multiplier	0.45	Controls the flow (amount) of the slurry while printing

Apart from the settings related to the physical setup, some of the settings related to the actual printing process that are tweaked are print speed, layer thickness, layer height, extrusion multiplier, etc based on the type of part that is printed. In addition, two more settings that are not controlled by the software but are important with regard to the quality of the prints are bed temperature and nozzle diameter. The bed temperature is controlled by using a simple hot plate on which the build platform is mounted and which is placed at the base of the printer as shown in Figure 2.2. The nozzle diameter can be changed/controlled by using plastic disposable nozzles of any desired size. Through experimentation, we have identified that most of the above-mentioned

settings need to be tweaked based on the type of part that is being printed and the quality of the batch of slurry that is being used. Although there is no fixed value that can be used, Table 4.1 shows the printing parameters that have been identified to have a significant effect on the print quality.

4.2 3D Printing of Ceramic Specimens

To understand the feasibility of using aqueous Zircon slurry as feedstock material for extrusion-based 3D printing, multiple samples were printed. Using CAD software PTC Creo Parametric, a 3D model of the desired geometry is developed. A model in STL format is extracted and uploaded to the 3D printing software Repetier Host. After the configuration of different print settings, the inbuilt slicer is used to generate the G-Code to define the tool path as per the geometry of the part. The batch of Zircon slurry is retrieved from the ball mill as shown in Figure 3.4 and loaded into the syringe. While loading the syringe with the slurry it is very important to make sure that there are no trapped air bubbles left, which can cause issues during the extrusion process. After loading the syringe, a nozzle of the desired size is attached and the syringe is then placed inside the extrusion cartridge. The extrusion motor with the linear actuator extruder is assembled on top of the cartridge and the entire extrusion assembly is placed into the customized mount. The printer setup with the completed assembly is shown in Figure 2.2. Also, before powering up the electronics it is important to make sure that the head of the extrusion screw of the motor is in proper contact with the syringe plunger so that no extrusion steps are missed when the print is initiated.

4.2.1 3D Printing of Thin-Walled Cylindrical Specimen

A thin-walled cylinder is chosen as the geometry to test the printability of the developed 3D printer system. This type of specimen is chosen as it is a simple shape and it forms a continuous geometry. As a result of this, when the slicing of the STL model is done the G-Code generated defines a continuous tool path for the 3D printer extruder. Since the current extrusion setup does not have a mechanism to arrest the flow of the slurry mid-extrusion, the closed geometry, and the continuous tool path helps to achieve a good quality print. (Shiyan Tang et al,2019)[24] in their study regarding 3D printing of alumina identified that ~50 vol.% of solid loading allows sufficient strength to maintain the constructed structure. Also, through their experiments they identified that

the processing parameters that affect the formation process in the order: solid loading > layer height > print speed > nozzle diameter[24]. Similarly other studies based on layered formation of near net shape ceramic parts for a highly loaded alumina slurry it is found that ideal slurry viscosity for optimal printing parameters is in the range of 8 and 20 Pa.s[22].

Through application of similar approach as demonstrated in above mentioned research studies for alumina slurries, the ideal zircon slurry composition is obtained by experimenting with different slurry compositions and trying test prints to achieve a slurry with viscosity that produces a good quality print. To perform this experiment multiple batches of slurry 200 gm total mass each were prepared using different component compositions. Through these experiments we observed that for zircon with particle size 0.1-0.7 microns and ~60 vol% solid loading yields a stable slurry suitable to be used as 3D printer feedstock. Further using a Bholin CVO Rheometer, viscosity for the ~60 vol% solid loading slurry was measured and observed to be in the range of 30 Pa.s. For the viscosity tests a cone geometry too with 40 mm diameter and a cone angle of 4° is used and shear rates (1/s) ranges from 0.1 Hz to 10 Hz. Figure 4.1 show the results for the instantaneous viscosity for the ~60 vol% solid loading zircon slurry.

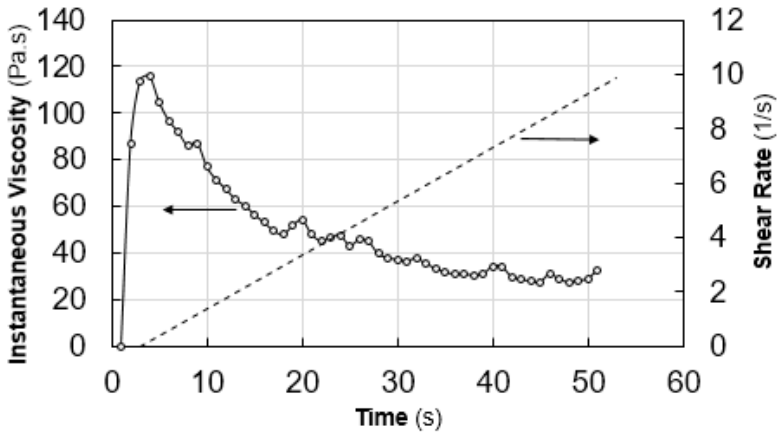

Figure 4.1: Viscosity Measurements, ~60 vol% Solid Loading Zircon Slurry

To stabilize and optimize the printing process in terms of improved print quality, test prints were performed using different slurry compositions and controlling different printing parameters. For these test print the print speed and layer height are kept constant at 8 mm/s and 0.7% of nozzle

diameter respectively. Table 4.2 lists the different slurry compositions in terms of vol% and the different printing parameter settings used for each batch for the print trials. Further, the result of the printed sample are shown in Figure 4.2

Table 4.2: Zircon Slurry Compositions and Printing Parameters for Process Optimization.

Batch No	Zrircon vol%	PVP vol%	Darvan rvol%	DI water vol%	Nozzle Diameter (mm)	Bed Temperature (°C)	Extrusion multiplier
1	56.56	4.73	3.18	35.53	2	25	0.5
2	60.47	4.31	2.79	32.43	2	25	1
3	58.85	4.47	3.03	33.65	1	25	1.5
4	59.52	4.25	2.76	33.48	0.5	60	0.7
5	59.51	4.25	2.73	33.51	2	60	1
6	59.50	4.24	2.75	33.51	1	60	0.5
7	60.07	4.18	2.86	32.89	0.5	70	0.45

Figure 4.2: Print Results for Different Slurry Compositions and Printing Parameters

Based on the results observed by comparing the trial prints for different slurry batches as seen in Figure 4.2, the composition of Batch 7 provided with the best quality prints. Using this as a reference for ideal slurry composition, the printing parameters listed in Table 4.1 were tweaked to successfully print a good quality specimen of a thin-walled high aspect ratio cylinder as shown in Figure 4.3 (b). From these results, we can observe that by controlling the slurry composition and the printing parameters we can improve the resolution of the print in terms of good layer formation and validate the integrity of the feedstock material to withstand multiple subsequent layering.

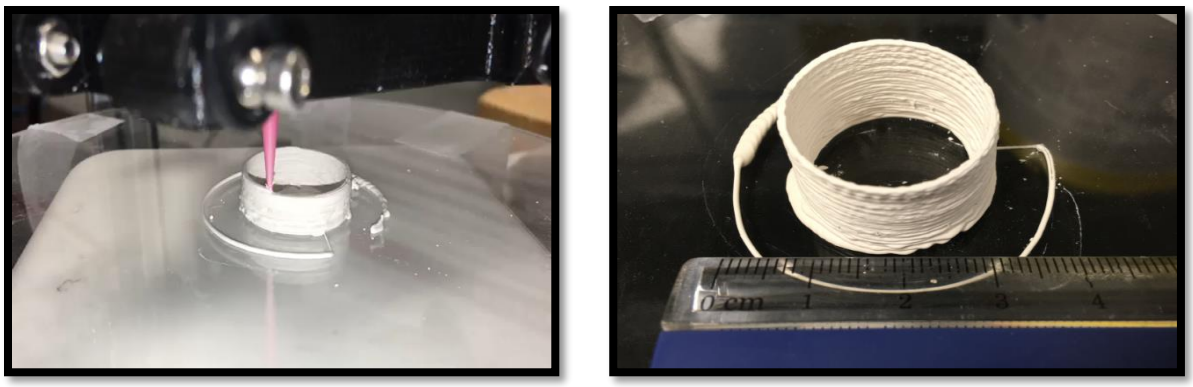

Figure 4.3: Results of Thin-Walled High Aspect Ratio Cylinder (a) Part Under Printing, (b) Printed Specimen

4.2.2 3D Printing of Biomimetic Inspired Honeycomb Specimens

After successfully printing a specimen with continuous simple geometry, possibilities of printing complex shapes are explored. In this study, the term complex shapes refer to a part with a geometry which upon slicing does not generate a G-Code depicting a continuous tool path for the extruder. To explore this capability of the printing system, the concept of biomimetic design is used. Based on this a simple symmetric honeycomb structure is selected as the geometry for the print trial. A cylinder with a hexagonal lattice structure is modeled using CAD software. The STL file for this part is imported to Repetier Host and sliced to generate the G-Code for this part. Figure 4.4 (a), shows the sliced model for the same. As mentioned earlier since the current extrusion

system lacks a mechanism to stop the flow of slurry during extrusion, printing of parts that require the return motion of the extruder without material deposition is currently not possible. However, by adjusting some of the printing parameters we are able to print a very thin layered cylinder as shown in Figure 4.4 (b), thus showing proof of concept that with further modification to the extrusion system even complex shapes can be successfully printed.

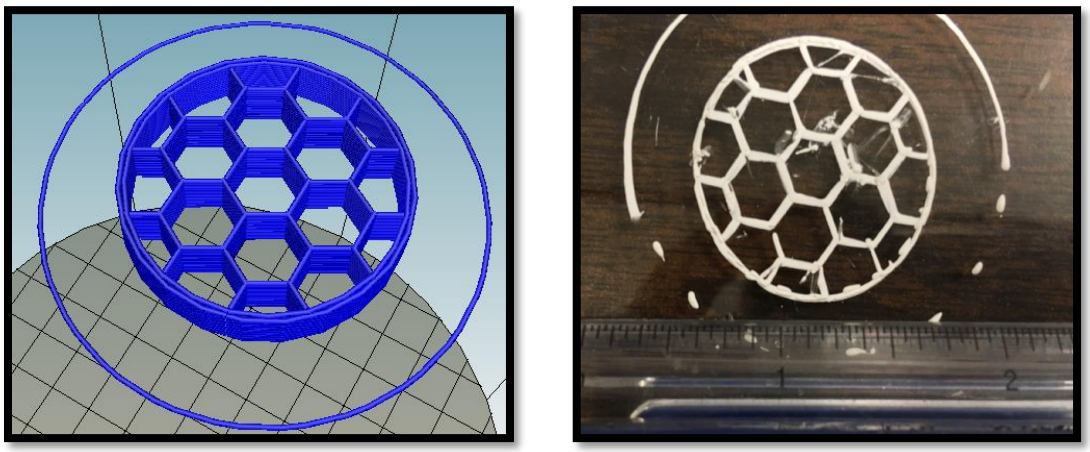

(a) (b)

Figure 4.4: 3D Printing of Complex Structures: (a) Sliced Model of Honeycomb Cylinder, (b) 3D Printed Ceramic Honeycomb Specimen

4.2.3 3D Printing of Mold Specimens

One of the primary advantages of developing Zircon as a 3D printing material is the ability to utilize its refractory and other properties and apply additive manufacturing technology for the production of molds. Apart from the beneficial properties of the material, the 3D printing process can be developed and calibrated to provide quick and easy means of production while adhering to the quality requirements in terms of dimensional accuracy which is one of the major requirements of the casting industry. Under the scope of this study, we have developed a small scale specimen of a mold by 3D printing and demonstrated the feasibility of using this process to cast a part using solder metal.

For this experiment, a solid model representative of a simple turbine blade geometry is developed using PTC Creo Parametric. The STL model for this part is extracted and uploaded to

Repetier Host which is sliced and a G-Code for this part is generated. A zircon slurry ~ 60 vol% is prepared and loaded into the extrusion system. After adjusting the necessary print settings, a single-walled specimen of the turbine mold is 3D printed successfully. Figure 4.5 (a) shows the 3D printed turbine mold specimen.

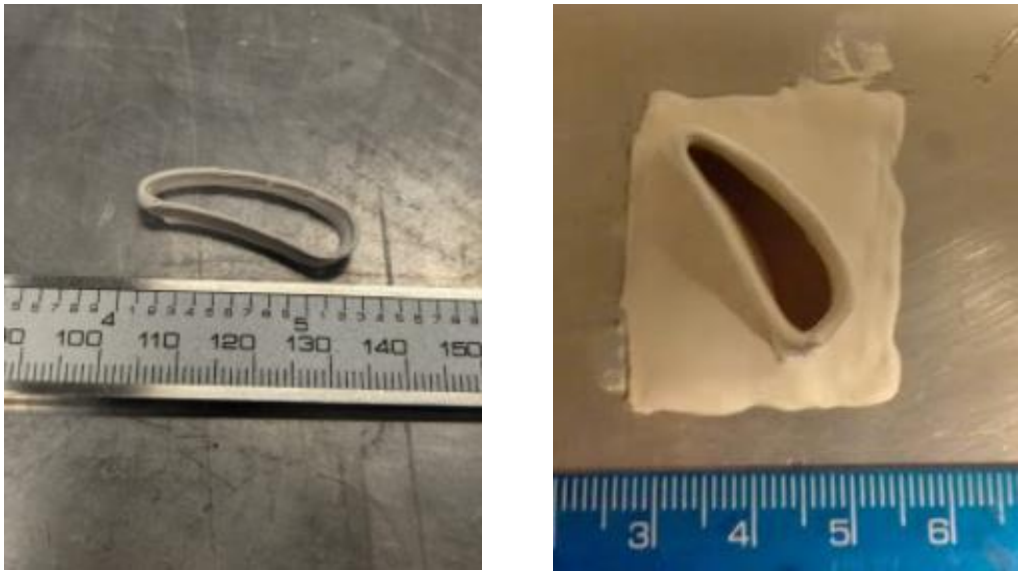

(a) (b)

Figure 4.5: (a) 3D Printed Mold Sample for Turbine Blade without Base, (b) Turbine Blade Mold Sample with Base

It is to be noted here that the mold specimen is printed without a base to reduce the time required for the completion of the print. A flat base for the mold is created separately using the same slurry and the 3D printed mold is placed onto this base just as it cures and solidifies as shown

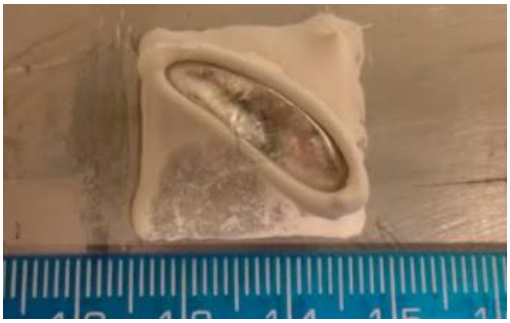

Figure 4.6: Turbine Mold with Solidified Solder Metal

in Figure 4.4 (b). Now to demonstrate the usability of this method for casting metal parts, solder metal consisting of Tin (Sn) and Lead (Pb) with a melting temperature of 360 °F is used. A small quantity of this metal is melted and poured into the mold to cast the turbine blade part as shown in Figure 4.6.

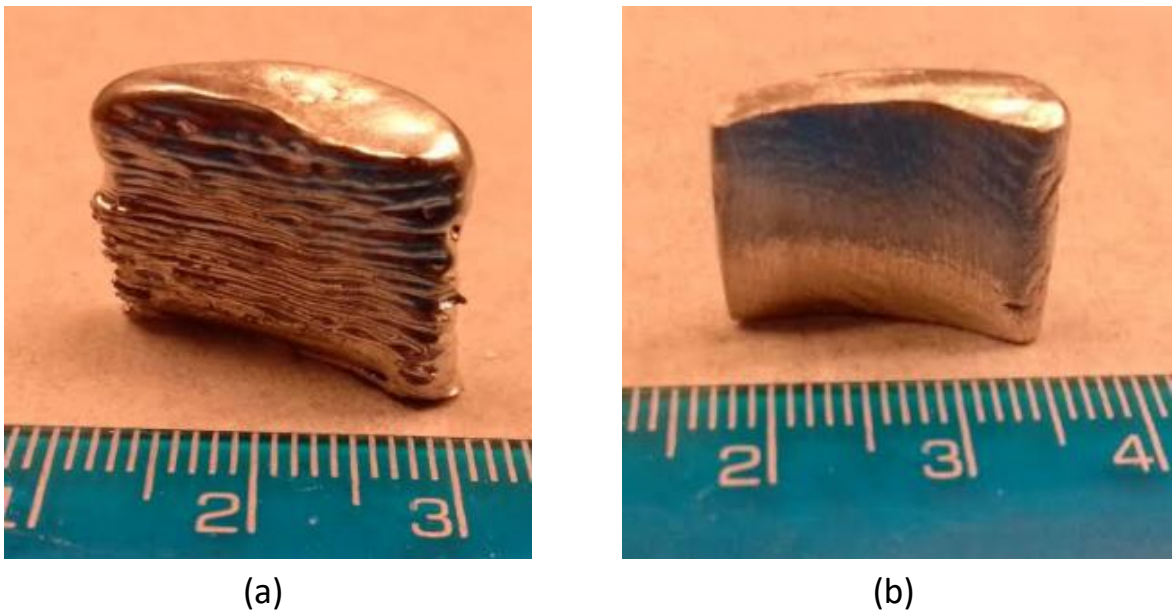

(a) (b)

Figure 4.7: Metal Part (a) Cast Metal Part with Rough Surface, (b) Cast Metal Part Post Surface Finishing

Once the solder metal solidifies, the mold along with the metal part is separated from the base. The mold is then broken and the cast part is extracted from the mold. Since the 3D printed mold is produced in a layer by layer fashion, the cast part develops this imprint on its surface and produces a part with a rough surface as shown in Figure 4.7 (a). To address this issue, surface polishing is carried out as a part of post-processing after which a finished part with a smooth surface is obtained as shown in Figure 4.7 (b). In its current state there are multiple aspects of this process such as dimensional accuracy, etc. that are required to be developed further, from this study the potential of implementing the 3D printing technique for mold production using Zircon is successfully demonstrated. To improve the surface quality of the printed mold specimen, the printing parameters optimized by tweaking parameters like extrusion multipler, layer thickiness etc. the surface quality of the 3D printed mold was significantly improved as shown in Figure 4.8. Although the result of casting metal part using the improved surface quality mold are not presented,

the surface quality of the casted part is expected be significantly improved in correlation to the nature of the part that was obtained after casting using a rough surface quality mold as shown in Figure 4.7 (a)

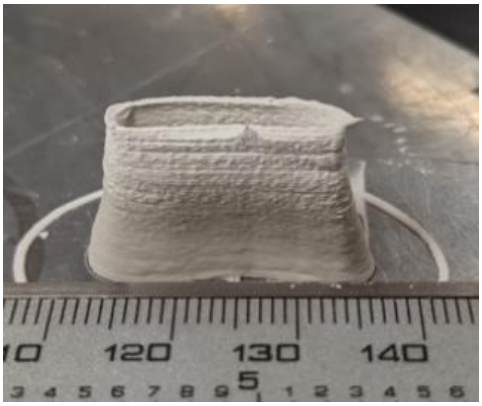

Figure 4.8: Improved Surface Quality 3D Printed Mold Specimen

4.2.4 3D Printing of Alumina, Bioglass and Zirconia

In this study, to understand the compatibility of the formulated ceramic slurries with the extrusion based 3D printing system, test samples were printed using the alumina, bioglass and zirconia slurries. As described in Section 4.1 and the beginning of Section 4.2, the formulated slurries were extracted from the ball mill and carefully loaded into the extrusion system and the printer was calibrated and setup to print the test samples. A C-Ring geometry is modelled using PTC Creo Parametric CAD software and the geometry model is extracted in the .stl format and the G-Code for this model is generated using Repetier Host software. C-Ring geometry is chosen as it has a simple design and can be used as a specimen for material testing. Figure 4.8 (a), (b), and (c)[15] show the print results for each of the ceramic slurry material namely Alumina, Bioglass and Zirconia respectively.

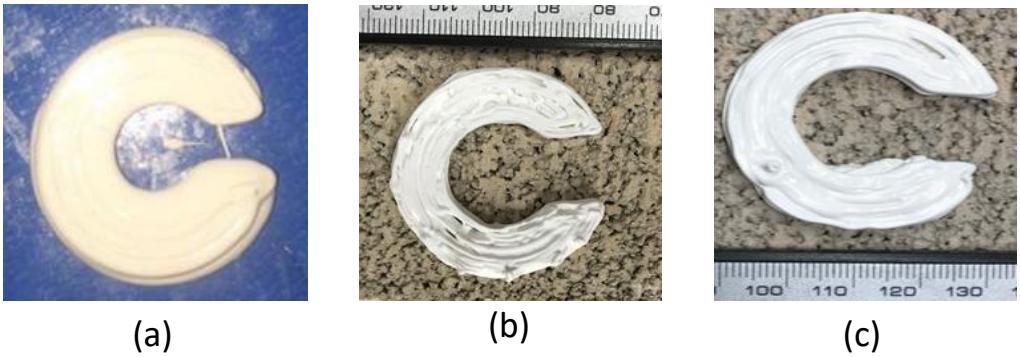

Figure 4.9: 3D Printed Test Specimen (a) Alumina, (b) Bioglass, (c) Zirconia

4.3 Material Testing Results

4.3.1 Heat-Treatment of Zircon Samples

In order to study the effects of heat-treatment on the Zircon samples, multiple square shaped samples were prepared. These samples were allowed to be dried by air quenching at room temperature prior to the heat-treatment process. In this study a Benchtop 1100°C Muffle Furnaces (Thermo Scientific™ Thermolyne™), is used to heat treat the samples at various temperatures. Each of the zircon sample was subject to a temperature profile of heating at 5°C /min and an isothermal hold at the target temperature for 60 minutes. After the isothermal hold period at the set temperature, the samples were again air quenched and then these samples were used for

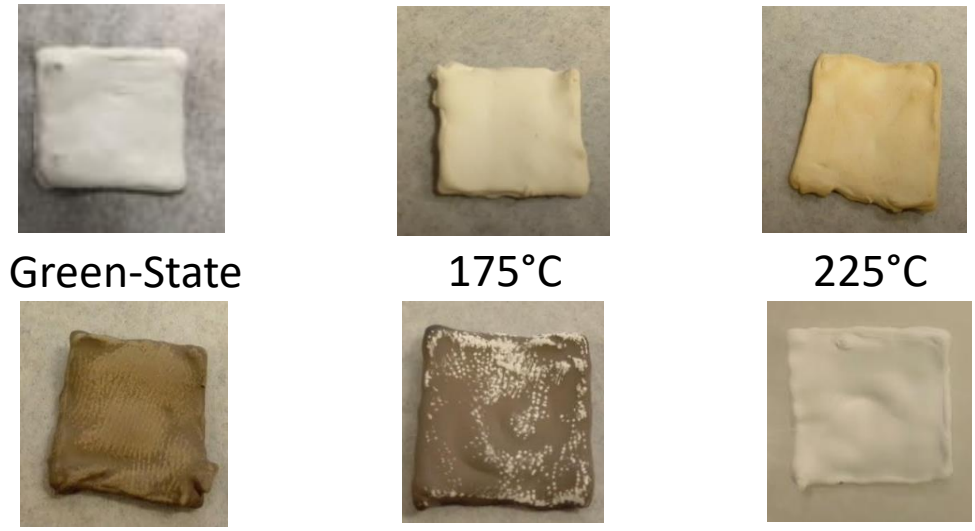

Figure 4.10: Zircon Samples at Different Heat-Treatment Temperatures

material testing to understand the effect of heat-treatment on the zircon samples. Figure 4.11 shows the zircon samples post heat-treatment at various temperatures. The samples are exposed to the lower range temperatures of up to 225°C to remove the moisture. Further at temperature ranges of up to 425°C the sample is expected to go through the binder burnout process. And the highest exposure temperature of 1100°C is chosen to study if there is any new grain growth and densification in the sample. The samples heat-treated at 225°C, 325°C, and 425°C show change in color post the heat-treatment process. This change in color is thought possible due to the binder and the deflocculant decomposition and depositing on the surface of the heat-treated sample

4.3.2 Hardness Testing, SEM and XRD Analysis of Zircon Samples

After the heat-treatment process is completed, the samples are used for hardness testing to understand the effect of heat-treatment. Vickers hardness test is performed to measure the micro-hardness of the Zircon samples and compare the effective changes between green-state and heat-treated sample. To perform the hardness test Model 900-391, Phase II (Upper Saddle River, NJ, USA) with pyramidal Vickers-type indenter is used. Each sample was indented on the top surface with the pyramidal indenter at a load of 1.96N with a dwell period of 15 seconds.

Each sample is tested 5 times by indenting different parts of the sample to determine the standard deviation for the micro-hardness value. Figure 4.11 shows results for all the samples of the Vickers Harness test. From the data it can be observed that initially as the heat-treatment temperature increases there is an increase in the microhardness value of the Zircon sample. Initially a gradual increase can be observed in the hardness value of the Zircon sample with increase in heat-treatment temperature up to 225°C followed by a sharp decrease in the hardness value of the

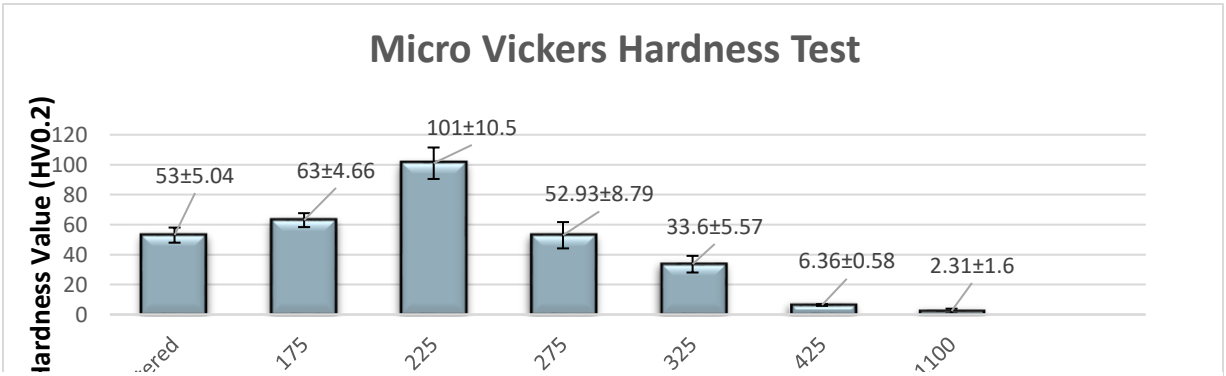

Figure 4.11: Vickers Hardness Values for Zircon Samples

sample. The initial increase of the sample can be possible due to the densification of the structure as the binder and deflocculant start to decompose as they reach their melting points. The decrease in the hardness value beyond 225°C can be possible due to the complete decomposition and evaporation of the binder and deflocculatnt and DI water from the sample structure which causes the formation of micropores in the structure. This porous structure is shown in the SEM analysis images for the heat-treated Zircon samples.

Scanning Electon Microscopy (SEM) and X-Ray Diffraction analysis are performed on the Zircon samples to study the effect of heat-treatment and the results are shown in Figure 4.12 - Figure 4.18. When the SEM images of samples are examined, it is possible to see that the microstructure is most dense at 225°C, which can be correlated to the peak in hardness value for the sample. However, as the heat-treatment temperature increases it can be observed that the microstructure starts becoming porous due to the loss of the binder, water and the deflocculant due to decomposition with maximum porosity at 1100°C as can be seen in Figure 4.18

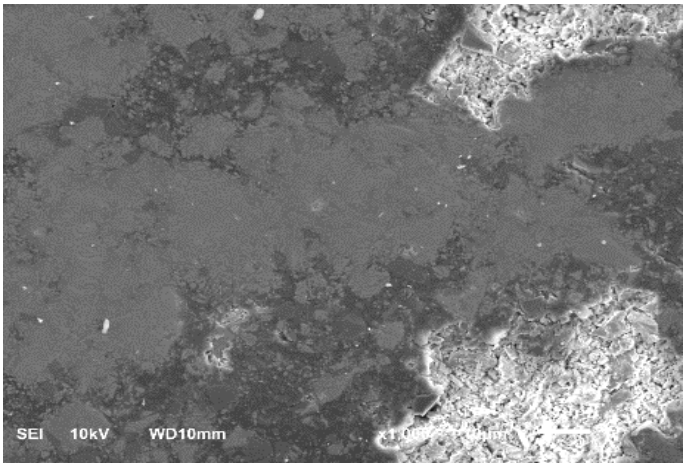

Figure 4.12: SEM Image of Green-State Zircon Sample

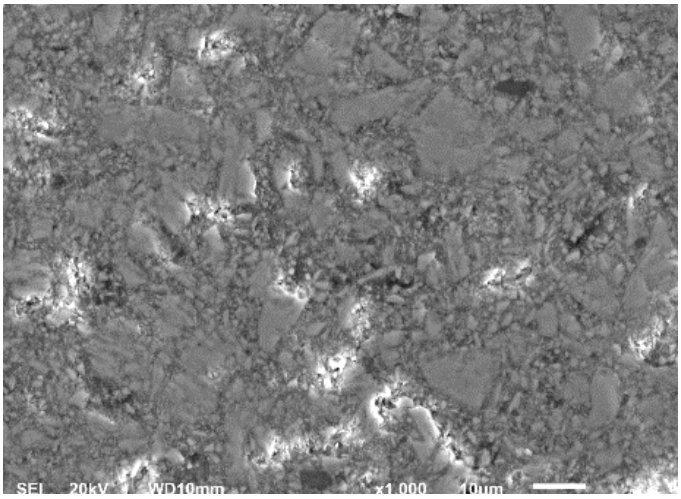

Figure 4.13: SEM Images Zircon Sample at 175°C

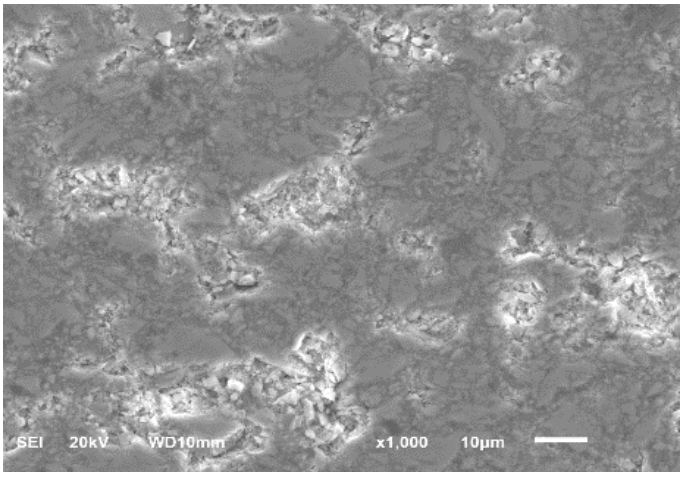

Figure 4.14: SEM Image Zircon Sample at 225°C

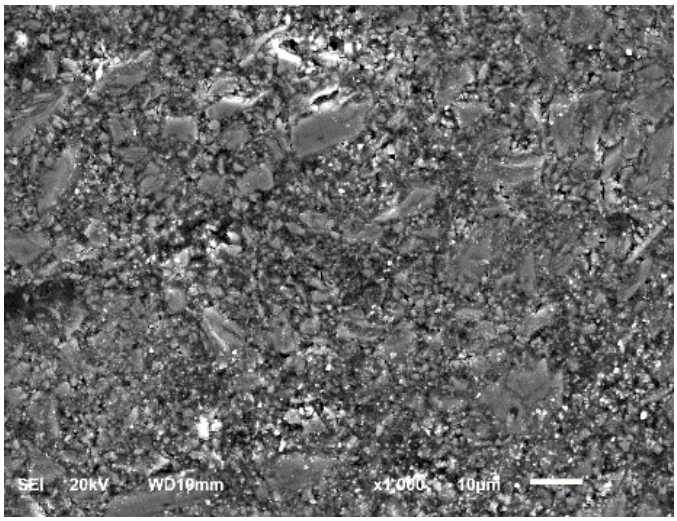

Figure 4.15: SEM Image Zircon Sample 275°C

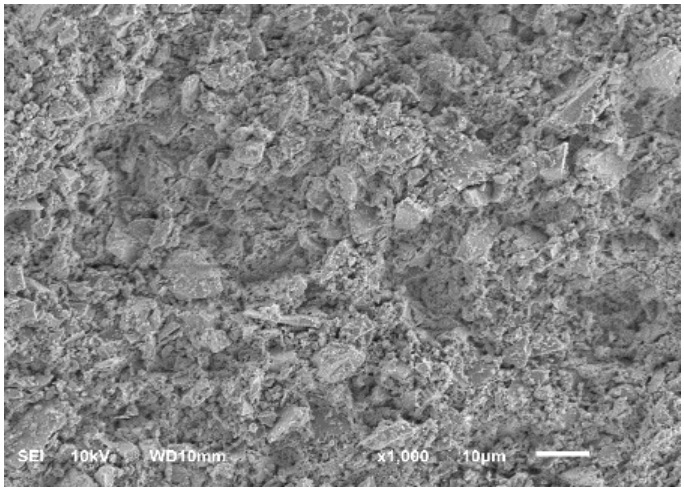

Figure 4.16: SEM Image Zircon Sample at 375°C

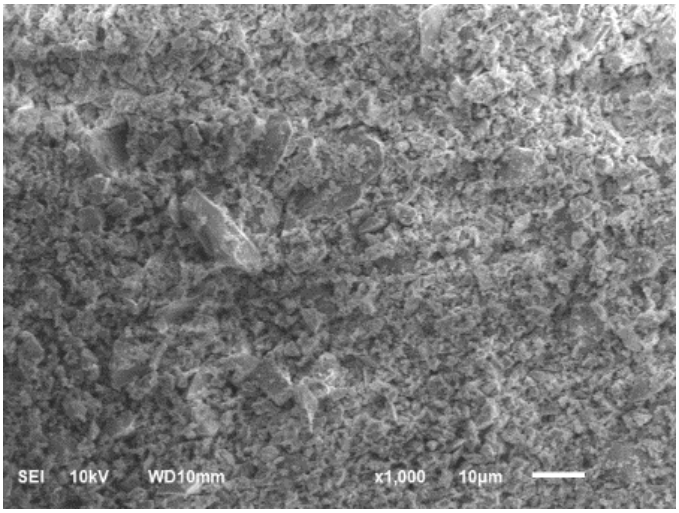

Figure 4.17: SEM Images Zircon Sample at 475°C

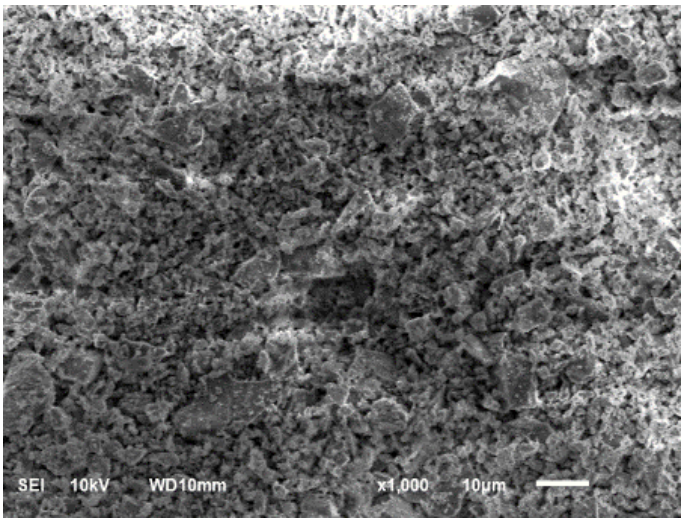

Figure 4.18: SEM Image Zircon Sample at 1100°C

X-Ray Diffraction (XRD) analysis of all the heat-treated and green-state Zircon samples is performed to identify how the phase of the material is effected by the heat-treatment process. Figure 4.19 shows the XRD analysis for the Zircon samples heat-treated at different temperatures. The XRD pattern in identified and peak intensities are marked as Zircon[25]. As can be seen from the results the XRD pattern for all the samples remains same for green-state as well as heat-treated samples. This indicates that the formulated slurry material is stable and there is no new material

formulation due to the heat-treatment in the observed temperature range. This results also correlate with material inherent behavior of high thermal stability and chemical inertness up to a temperature of 1673°C[13].

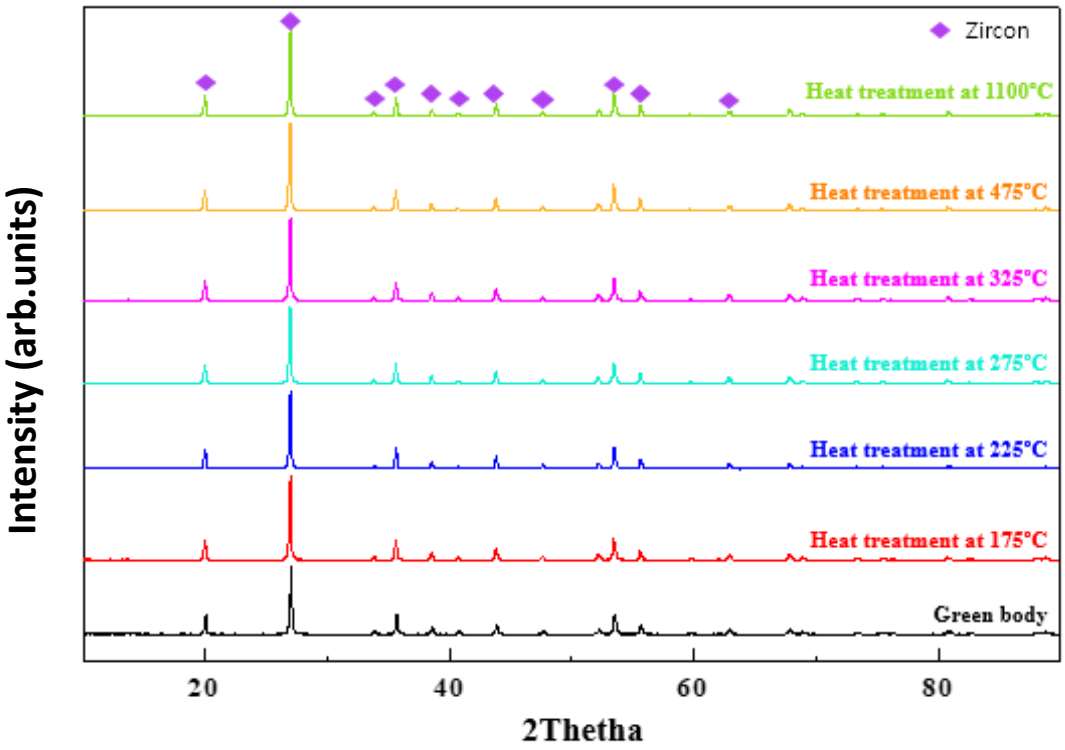

Figure 4.19: XRD Patterns for Zircon Samples at Different Heat-Treatment Temperatures

4.3.3 Heat-Treatment Study of Alumina, Bioglass and Zirconia Samples

To understand the effect of heat-treatment, a tube furnace (VTF-1700-100X300mm, Shanghai Alarge Furance Co., Ltd, China) is used to heat-treat the C-Ring samples of alumina, bioglass and zirconia. The alumina and the zirconia samples were subjected to a temperature of 1100°C and the bioglass samples were subjected to a temperature of 500°C. For each of the samples a similar temperature profile was used, a 60-minute elevation followed by a 60-minute isothermal hold period at their respective heat-treatment temperatures[15]. Figure 4.20 (a), (b), and (c) show the post heat-treated samples for Alumina, Bioglass and Zirconia respectively. When analyzed it was observed that the samples experienced some shrinkage with respect to the diameter of the samples approximately in the range of ~1 mm,~2mm and ~4mm for Alumina, Bioglass and

Zirconia samples respectively[15]. Vickers hardness test was done to measure the microhardness values of the 3D printed ceramic specimens. It was observed that the hardness value increased from 37±3 to 112±5 HV0.2 for Alumina, 22±5 to 31±3 HV0.2 for Zirconia, and 23±5 to 35±1 HV0.2 for Bioglass, for green-state and heat-treated samples[15]

Figure 4.20: Heat-Treated Specimen (a) Alumina, (b) Bioglass, (c) Zirconia

5. MODEL BASED SYSTEM ENGINEERING APPROACH FOR CERAMIC 3D PRINTER SYSTEM DESIGN

5.1 Introduction

System Engineering (SE) as defined by International Council Of System Engineers is a transdisciplinary and integrative approach to enable the successful realization, use, and retirement of engineered systems, using systems principles and concepts, and scientific, technological, and management methods[26]. It focuses on holistically and concurrently understanding stakeholder needs; exploring opportunities; documenting requirements; and synthesizing, verifying, validating, and evolving solutions while considering the complete problem, from system concept exploration through system disposal[26]. One of the newer and more popular approach to apply the system engineering principles to a product or system development process is Model-Based Systems Engineering (MBSE). MBSE is the formalized application of modeling to support system requirements, design, analysis, verification, and validation activities beginning in the conceptual design phase and continuing throughout development and later life cycle phases[27]. In order to implement the MBSE approach, various system modelling tools can be used. These tools are developed on the basis of System Modelling Language (SysML) which is a modeling language that is used develop a System Model that is capable to support the analysis, specification, design verification, and validation of any complex system[28].

In this study, Cameo Systems Modeler a SysML tool developed by NoMagic is used for the modeling of the Ceramic Manufacturing System. To implement all the processes defined in the SE process, a framework called as MagicGrid approach developed by NoMagic is used. Figure 5.1 shows the MagicGrid framework matrix that captures the different system domains and the four pillar of SE respectively. As can be seen in Figure 5.1, each row of the matrix defines one of the domains of the system i.e. problem domain with the Stakeholder Needs Development process, solution domain with the Architecture Definition process, and implementation domain with the Design Definition process[29]. Further each of the columns defines the different aspects of the system i.e. Requirements, Behavior, Structure and Parameters (Parametric) which correspond to the four pillars of the SE process.

<table>
<tr><td></td><td colspan="6">PILLAR</td></tr>
<tr><td rowspan="8">DOMAIN</td><td colspan="2"></td><td>Requirements</td><td>Behavior</td><td>Structure</td><td>Parameters</td><td rowspan="8">Specialty Engineering

Integrated Testing

Analysis</td></tr>
<tr><td rowspan="2">Problem</td><td>Black Box</td><td rowspan="2">B1-W1 Stakeholder Needs</td><td>B2 Use Cases</td><td>B3 System Context</td><td>B4 Measurements of Effectiveness</td></tr>
<tr><td>White Box</td><td>W2 Functional Analysis</td><td>W3 Logical Subsystems Communication</td><td>W4 MoEs for Subsystems</td></tr>
<tr><td colspan="2" rowspan="4">Solution</td><td>S1 System Requirements</td><td>S2 System Behavior</td><td>S3 System Structure</td><td>S4 System Parameters</td></tr>
<tr><td>SS1 Subsystem Requirements</td><td>SS2 Subsystem Behavior</td><td>SS3 Subsystem Structure</td><td>SS4 Subsystem Parameters</td></tr>
<tr><td>...</td><td>...</td><td>...</td><td>...</td></tr>
<tr><td>C1 Component Requirements</td><td>C2 Component Behavior</td><td>C3 Component Structure</td><td>C4 Component Parameters</td></tr>
<tr><td colspan="2">Implementation</td><td>I1 Physical Requirements</td><td colspan="3">Software, Electrical, Mechanical</td></tr>
</table>

Figure 5.1: MagicGrid Approach Framework[29]

While modeling a system based on the MagicGrid framework, in the problem domain the analysis and refinement of the system requirements is performed in two phases. These phases define the modelling perspectives that should be incorporated while defining the system model ie. Blax Box and White Box. In the Black Box perspective, operational analysis is done on the system of interest (SOI) by focusing on its interactions with the environment without defining any of the internal structure or behavior. In the White Box perspective, functional analysis of the SOI is performed by focusing on how the system shall operate to achieve the desired results. Thus in the problem domain, through the functional analysis of the SOI the different subsystems can be identified and the system requirements for these subsystems can be defined. Further, the logical level architecture of the SOI can be developed as part of the solution domain. Similarly, the logical architecture can be defined for each subsystem and consequent subsystem based on the level of abstraction of the modelling effort. Finally, from the defined logical level architecture of the SOI and its subsystems, physical requirements or detailed technical specifications of each subsystem can be defined as part of the implementation domain. After this point the actual physical system is designed by engineering efforts and the SE effort as per the MagicGrid framework is arrested. Figure 5.2 shows the traceability between each aspect of the modelling process and the different types of SysML diagrams that are used in the modelling process.

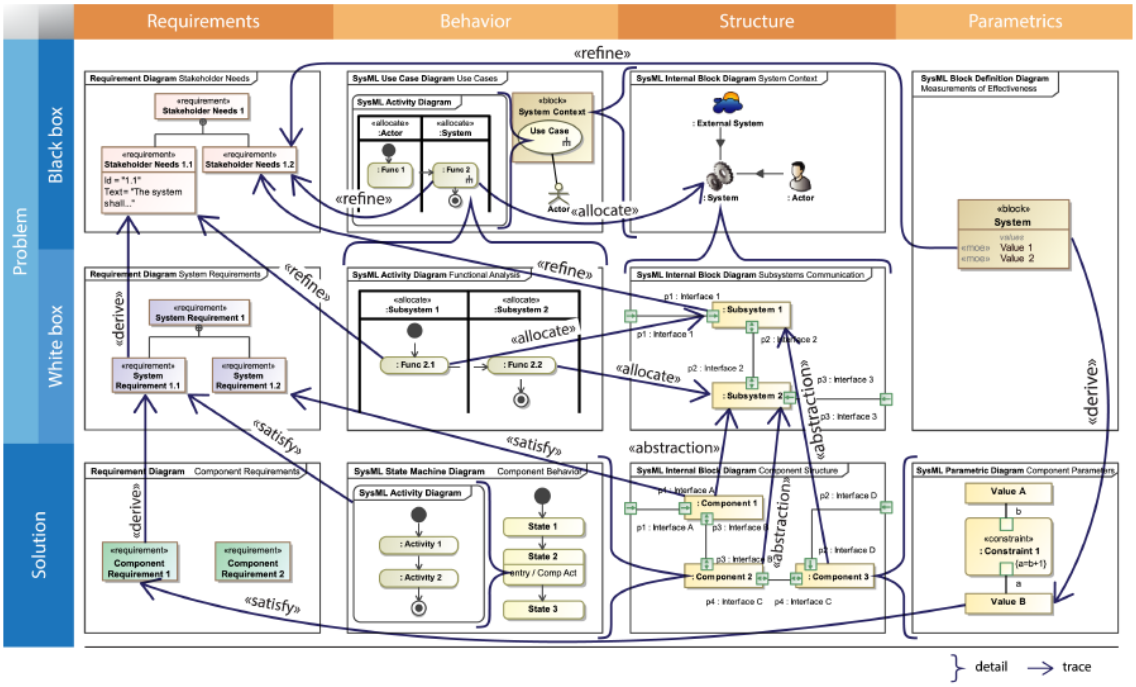

Figure 5.2: Traceability in MagicGrdig Matrix and Usage of SysML diagrams[30]

5.2 System Modeling of Ceramic 3D Printing System

5.2.1 Introduction

This chapter shows the details regarding the modeling of the Ceramic Manufacturing System through the implementation of MagicGrid framework using Cameo System Modeller tool. Figure 5.3 shows the entire model as captured in the MagicGrid framework matrix. It is to be noted here that the system model was developed based on a bottom up approach, which can constrain the development of multiple solution architectures or trade-off studies as the actual engineered system is already existing. Also, in this study only the functional aspects of the system are considered and the parametric pillar of the SE process is not defined.

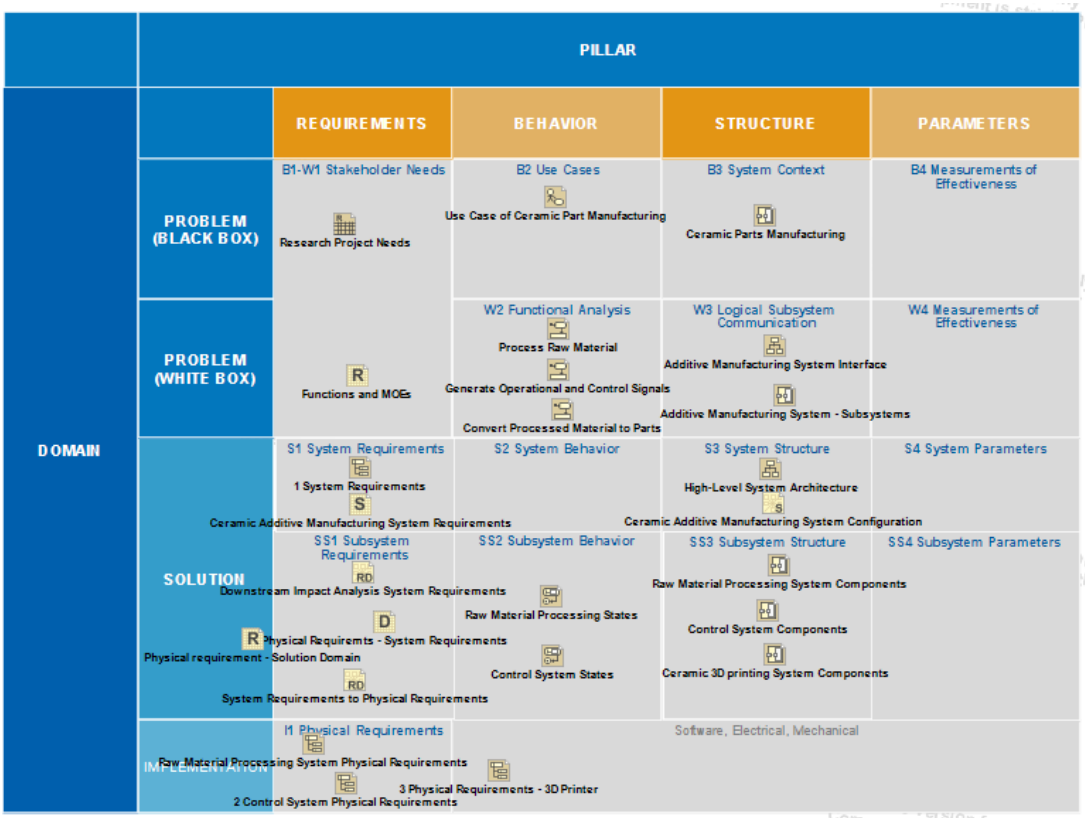

Figure 5.3: Ceramic 3D Printing System Model MagicGrid Matrix

5.2.2 Problem Domain Modeling - Black Box

As mentioned earlier, the problem domain of the system is split into two phases i.e. Black Box and White Box. The modelling process begins by capturing the stakeholder needs, which is done by using a requirements table or a requirements diagram. The different stakeholder needs such as need to use additive manufacturing process, using Zircon as the ceramic materials etc. are captured as can be seen in Figure 5.4. Next the system context for the SOI is defined. The system context is modeled using a internal block definition diagram (ibd) where the SOI and all the other system that interact with the it are captured using blocks. Figure 5.5 shows the different participants in the system environment.

#	Name	Text
1	1 Research Project Goal	
2	1.1 Engineering Ceramic Parts	Develop a manufacturing Process to produce ceramic parts.
3	1.1.1 Additive Manufacturing	The research project should leverage Additive Manufacturing Technology to produce ceramic parts.
4	1.1.2 Zircon (ZrSiO4)	Zircon (ZrSiO4) should be used as the material, due to its inherent properties.
5	1.2 System Complexity	The developed system should be technologically simple and economically efficient.
6	1.3 Applications of developed s	The developed system should be capable of producing parts that should include simple and complex shapes and geometries; and should have possible applications in mold manufacturing process.

Figure 5.5: Stakeholder Needs Ceramic Manufacturing System

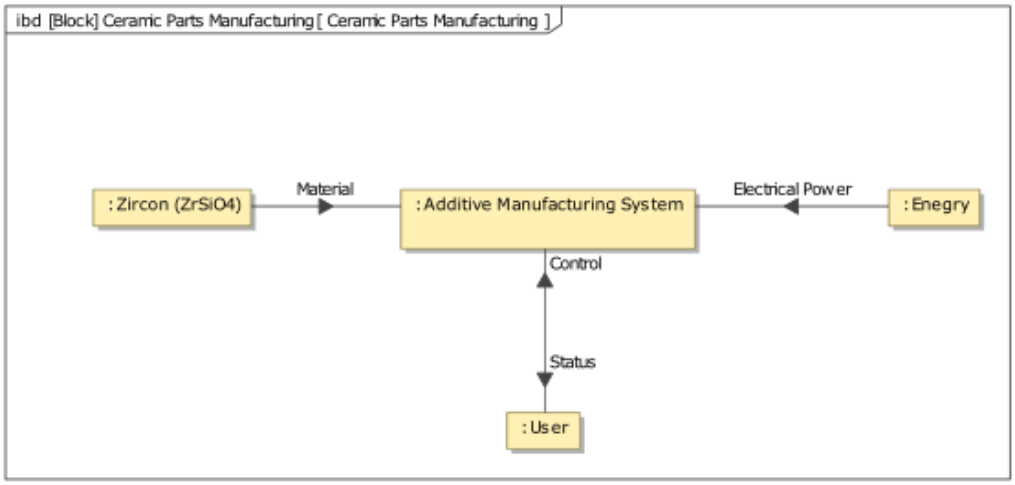

Figure 5.4: System Context Ceramic Parts Manufacturing System

Next step to further refine the stakeholder needs a use case of the SOI based on the system context is developed by using SysMl use case diagram. Figure 5.6 shows the use case diagram for the Ceramic Manufacturing System where a user interacts with the system to perform an activity called Additive Manufacturing of Ceramics. Further the activity Additive Manufacturing of Ceramics is modelled by using SysML activity diagram. As shown in Figure 5.7, through this diagram we capture all the steps or functions that are required to achieve the desired output from the SOI and assign them to the appropriate participants in the system context environment. From a logical level standpoint, we have captured three critical function namely process raw material, generate operational and control Signals, and convert processed material to parts and assigned them to our system of interest the Additive Manufacturing System by using swim lanes.

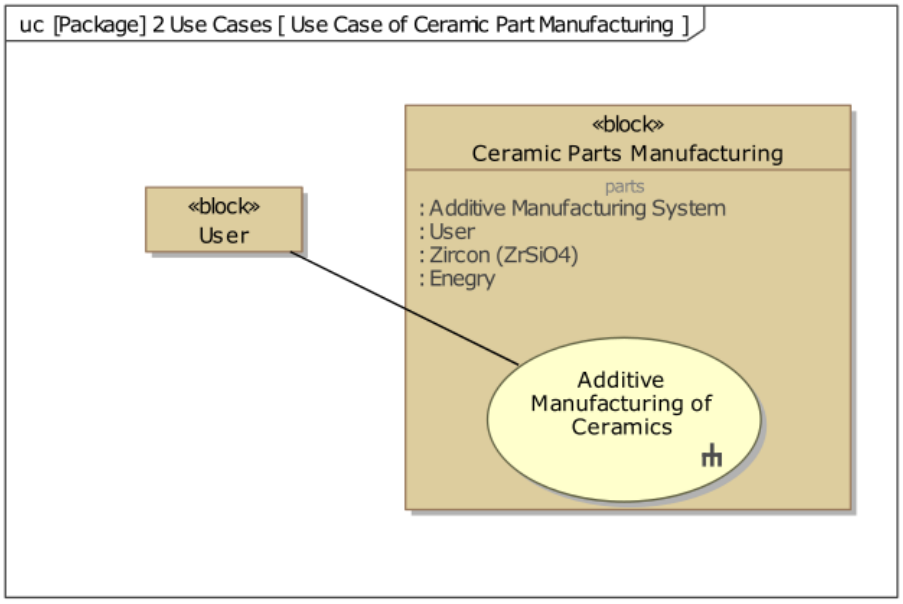

Figure 5.7: Use Case Diagram Ceramic Part Manufacturing Context

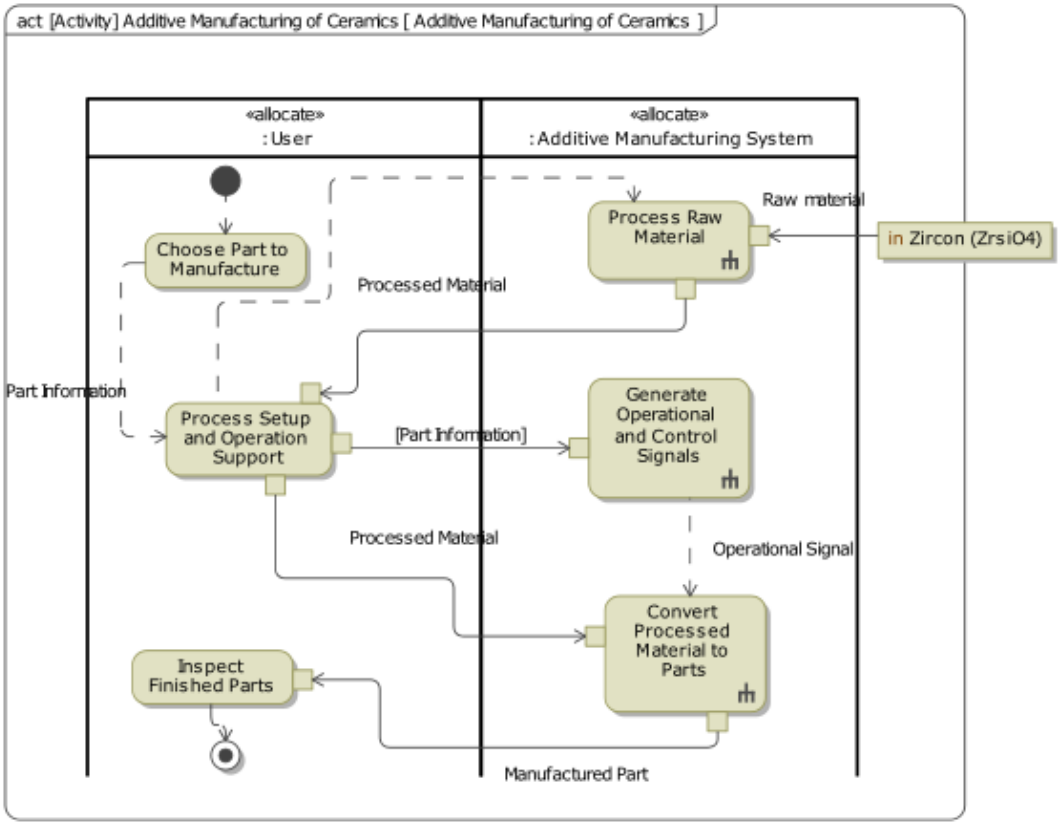

Figure 5.6: Additive Manufacturing of Ceramic Activity Diagram

5.2.3 Problem Domain Modeling – White Box

Once the system context and the high level functions of the SIO is captured the White Box perspective modelling of the system begins. This phase begins with further decomposing of the functions defined at the black box level. This is done by developing further logical level functions for each of the functions assigned to the SIO of interest as shown in Figure 5.7. For this model, this is done for all the three functions that are assigned to the Additive Manufacturing System which is our SOI. Figure 5.8 shows the logical level breakdown of the function Process Raw Material using an activity diagram. After completing the functional decomposition of the SIO, a SysML block definition diagram is used to capture the interfaces of the SIO. Here the flow of materials, signals, etc. are capture by using proxy ports and interface blocks. Figure 5.9 shows the interface diagram for the Additive Manufacturing System.

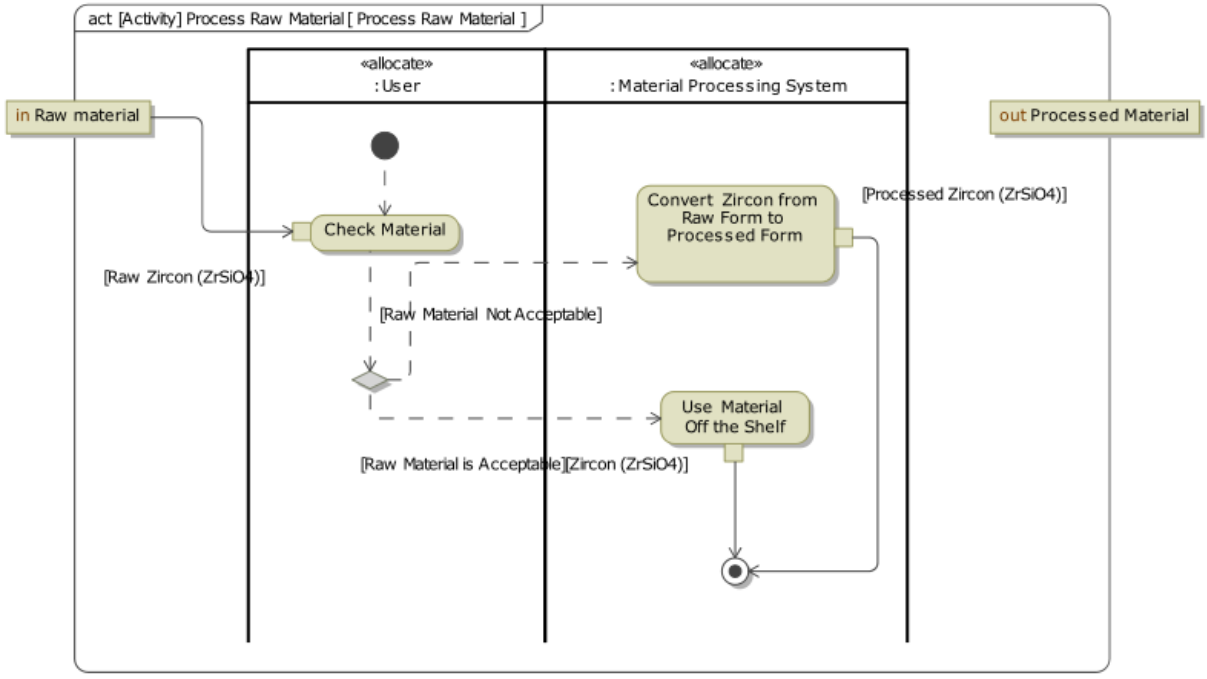

Figure 5.8: Logical Level Functional Decomposition of Process Raw Material Function

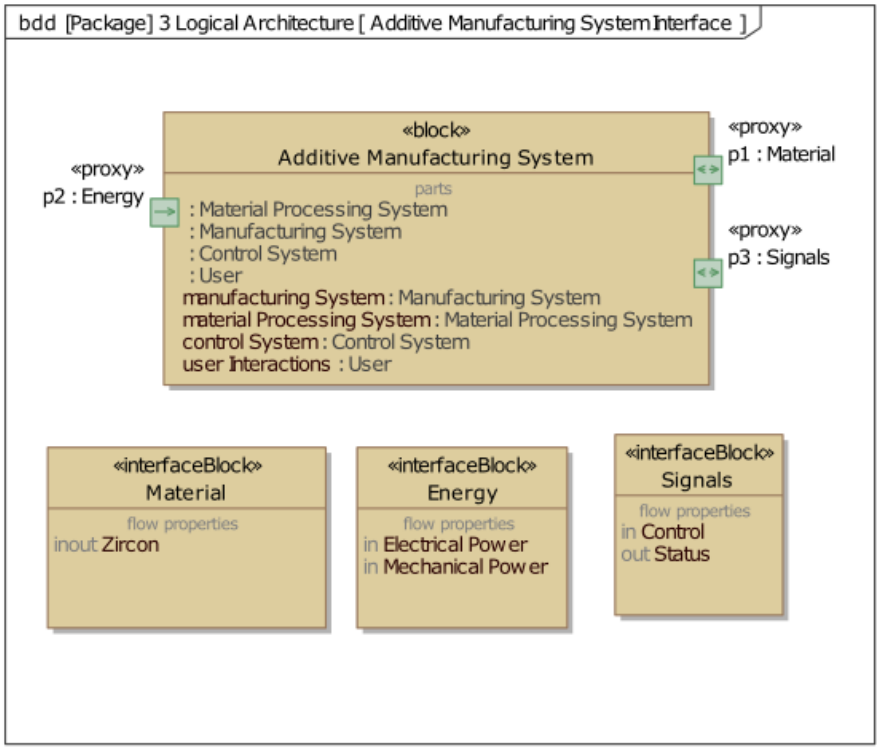

Figure 5.9: Ceramic Additive Manufacturing System Interface

Once the functional decomposition of the SIO is completed and the interfaces are defined, we can extract and model the logical subsystems of the SIO. This is done by creating an internal block definition diagram (ibd) for the Additive Manufacturing System block as shown in Figure 5.10. For our SIO the ibd consists of Material Processing System, Manufacturing System and Control System, with User defined as a block the interacts with all three subsystems. Also, all the interactions or flows between the subsystems and the SIO are captured by using proxy ports.

As the final step to complete the modelling for the problem domain of the system, traceability is defined for all functions captured in through the operational and functional analysis of the SIO in the Black and White Box phases respectively. Figure 5.11 shows a traceability matrix that captures the refine relationship between each of the logical level function and the stakeholder needs. This process helps to validate that each of the stakeholder needs is refined by at least one of the functions to avoid missing any critical requirement downstream, which can cause rework or project failure.

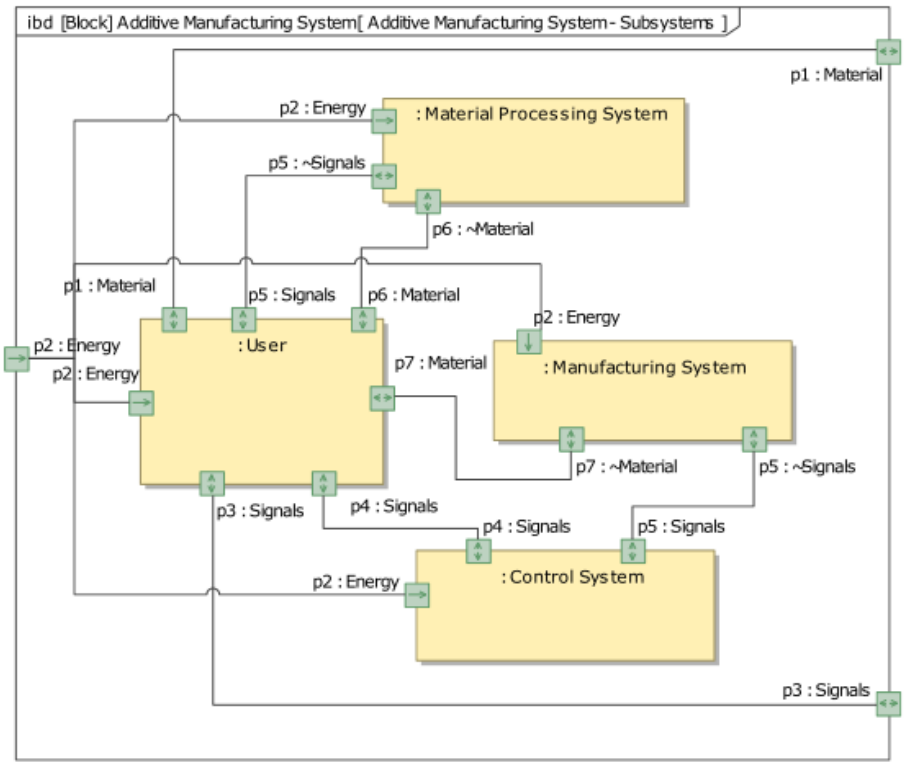

Figure 5.10: Ceramic Additive Manufacturing System- Subsystem

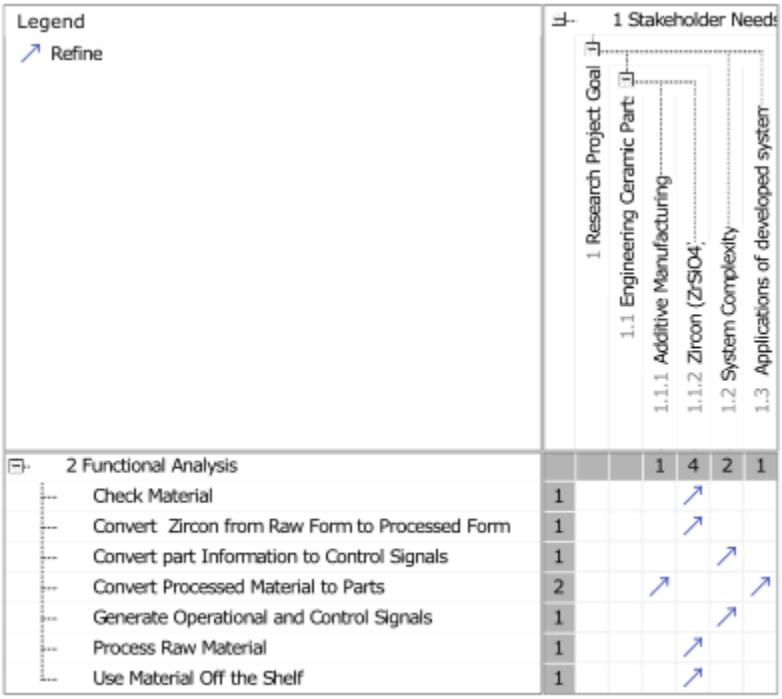

Figure 5.11: Functional Analysis Refinement Traceability Matrix

5.2.4 Solution Domain Modeling

Once the problem domain modelling of the system is completed, we can start working on the solution domain of the system. Here a detailed logical architecture of the SIO and the subsystem is modeled. The modelling in solution domain begins by developing system requirements based on the stakeholder needs and the functional analysis of the system in the problem domain. Figure 5.12 shows the system requirements captured for the SIO Additive Manufacturing System. A traceability matrix can be developed to define which system requirement is derived from which stakeholder need.

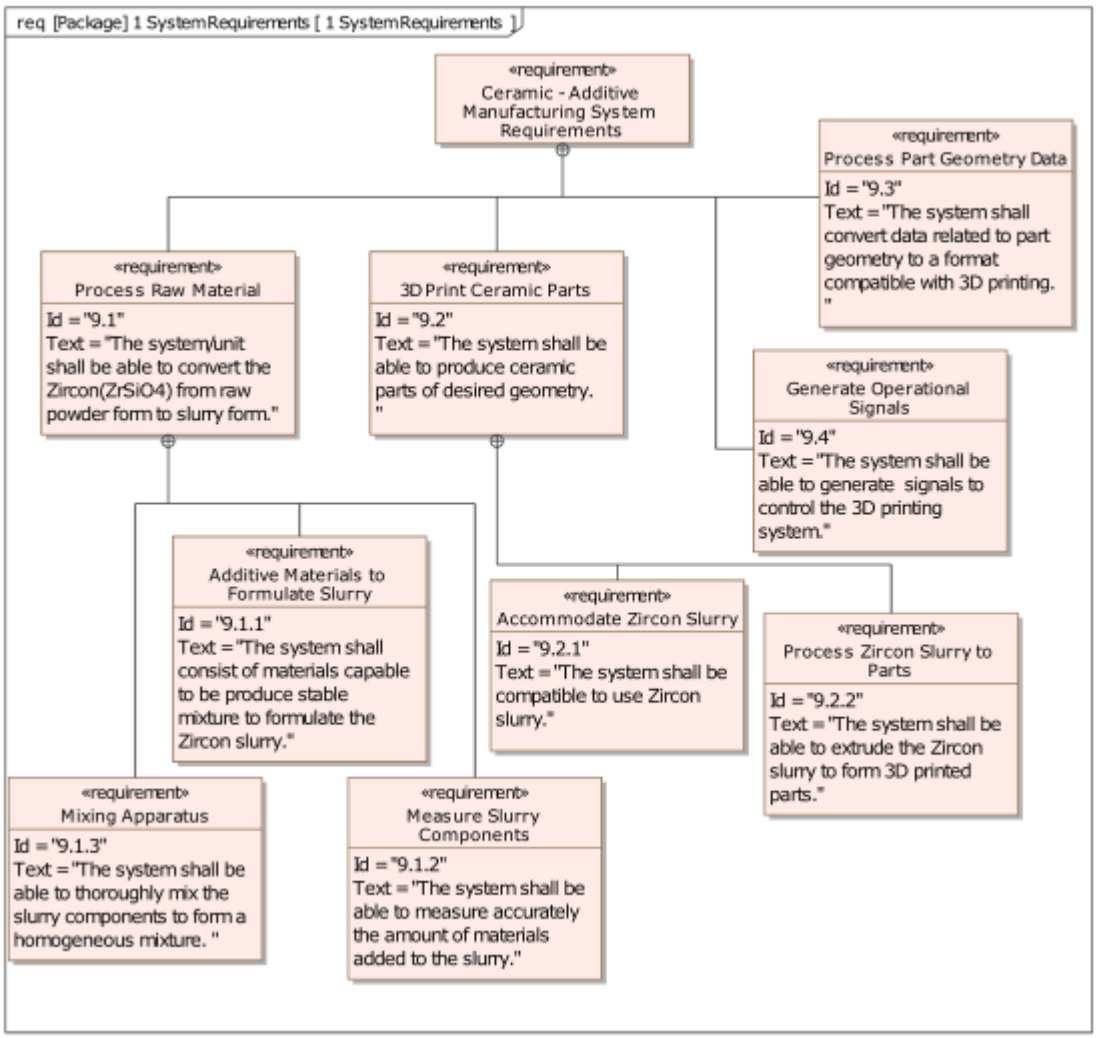

Figure 5.12: System requirements for Ceramic Additive manufacturing System

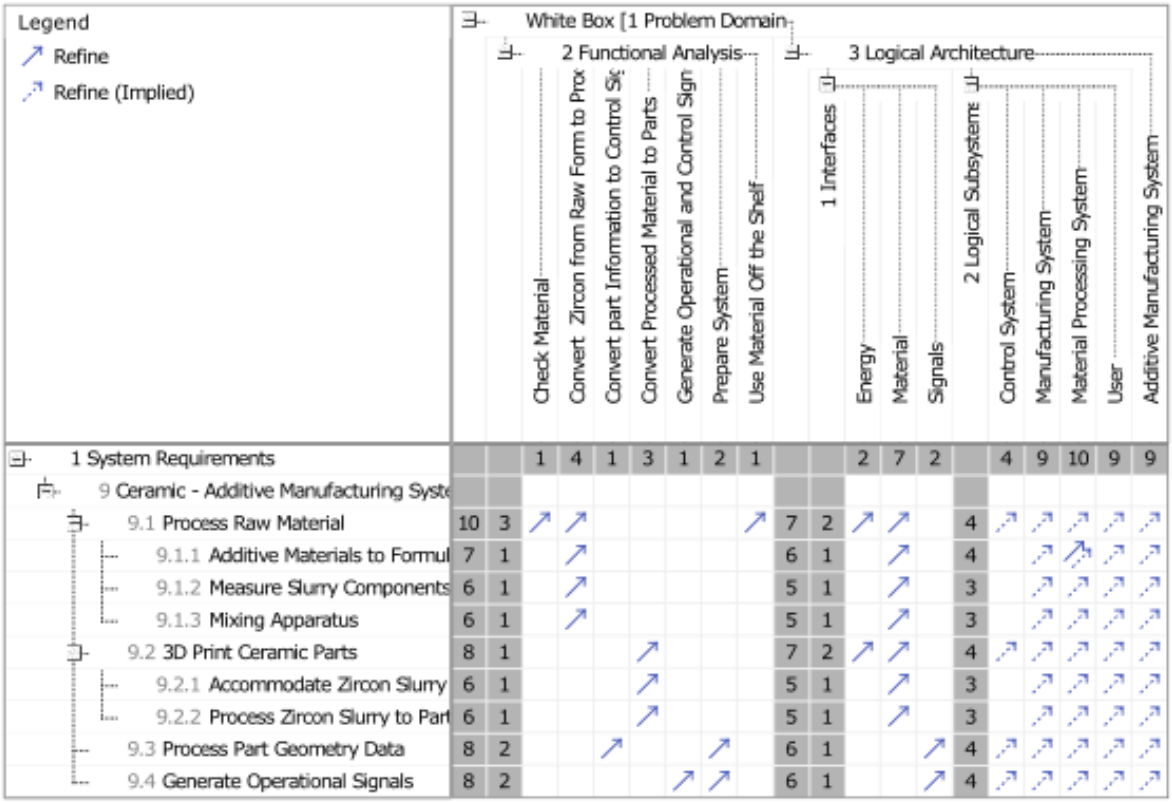

Figure 5.13: Traceability Matrix System Requirement – Problem Domain

Figure 5.13 shows the traceability between the System Requirements and the problem domain. This matrix shows which system requirement directly refines functional aspect of the system and also any other implied refine relationships with any of the logical level subsystems. Once the system requirements are captured and modelled, a high-level system architecture (HLSA) is modelled which captures all the subsystem of the system and defines the various flows through the subsystems of the SIO. A bdd is used to capture HLSA for the SIO, as shown in Figure 5.14. Further, an ibd is used to define the internal structure of the SIO and the interaction between the different subsystem as shown in Figure 5.15. Next traceability through abstraction relationships are modeled between the logical architecture in the problem domain to the HLSA of the SIO in the solution domain as shown in Figure 5.16.

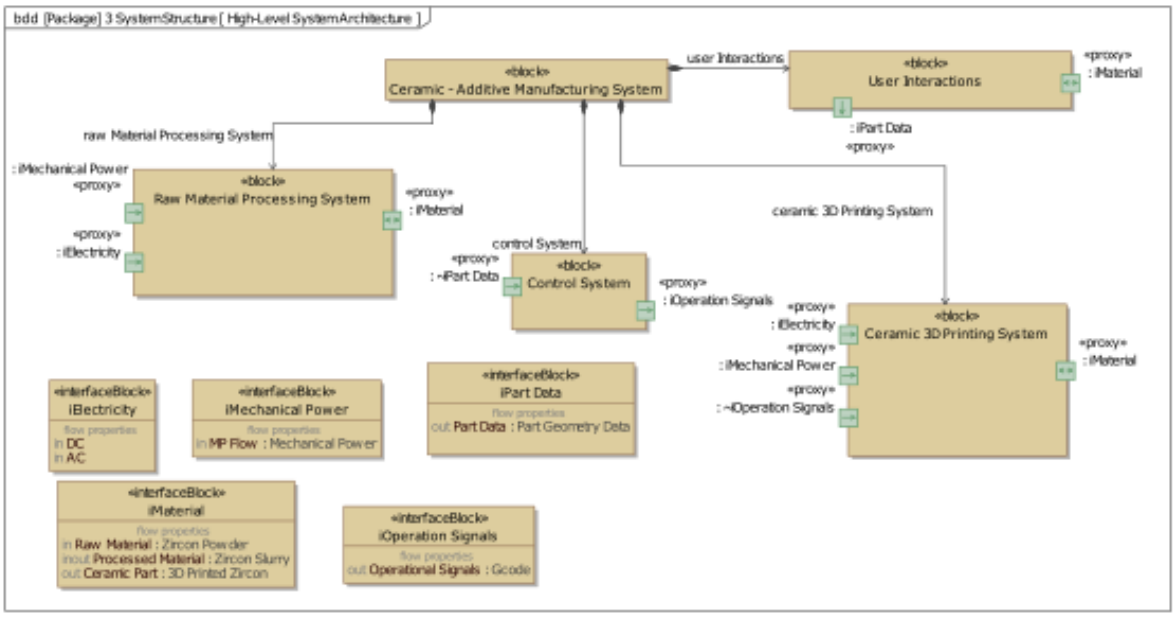

Figure 5.15: High Level System Architecture of Ceramic- Additive Manufacturing System

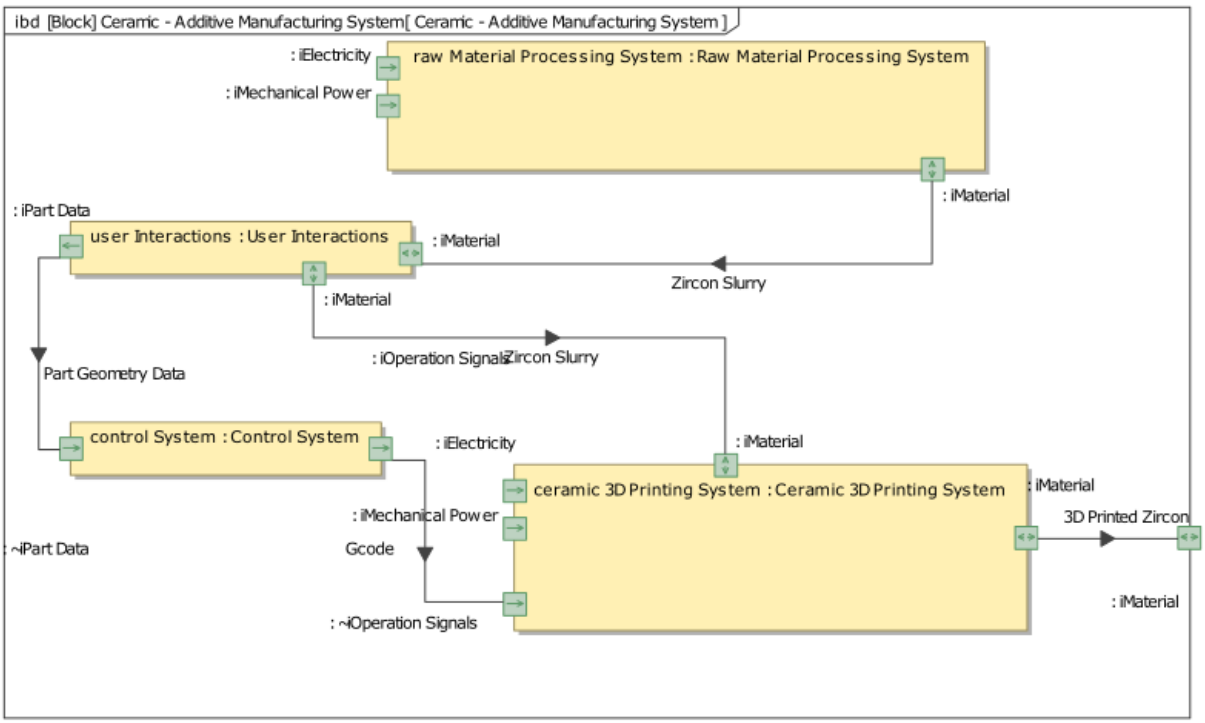

Figure 5.14: Internal Block Definition of Ceramic- Additive Manufacturing System

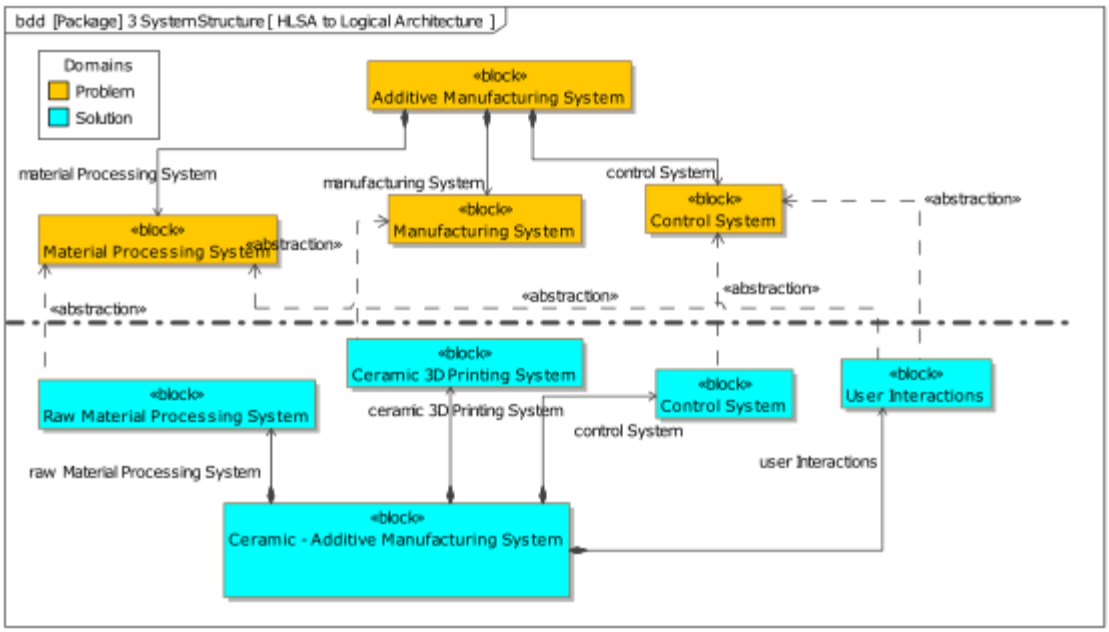

Figure 5.16: Traceability between Architecture (Problem Domain) and HLSA of SIO

Once the HLSA of the SIO is defined, the architecture of each of the subsystems can be modelled. For this SIO the three subsystems that are identified are Raw Material Processing System, Control System, and Ceramic 3D Printing System. Using SysMl ibd diagram the logical level structure architecture of the three subsystems is modelled. The different parts of these subsystems are identified based on the system requirements and the functional analysis of the system done previously. Figure 5.17; Figure 5.18; and Figure 5.19 show the internal structure architecture for Control System, Raw Material Processing System, and Ceramic 3D Printing System respectively. Also, the flow of materials and information between the different parts of each subsystem is captured in this stage.

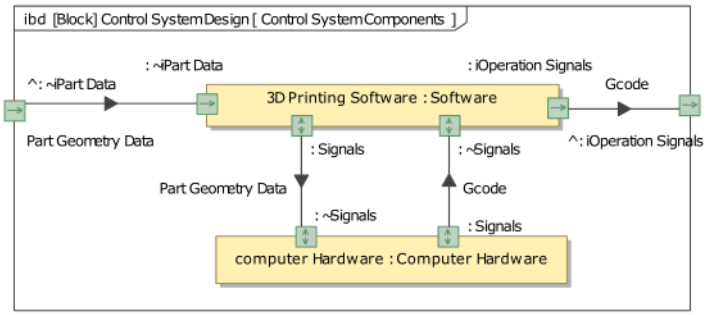

Figure 5.17: Logical Architecture of Control System

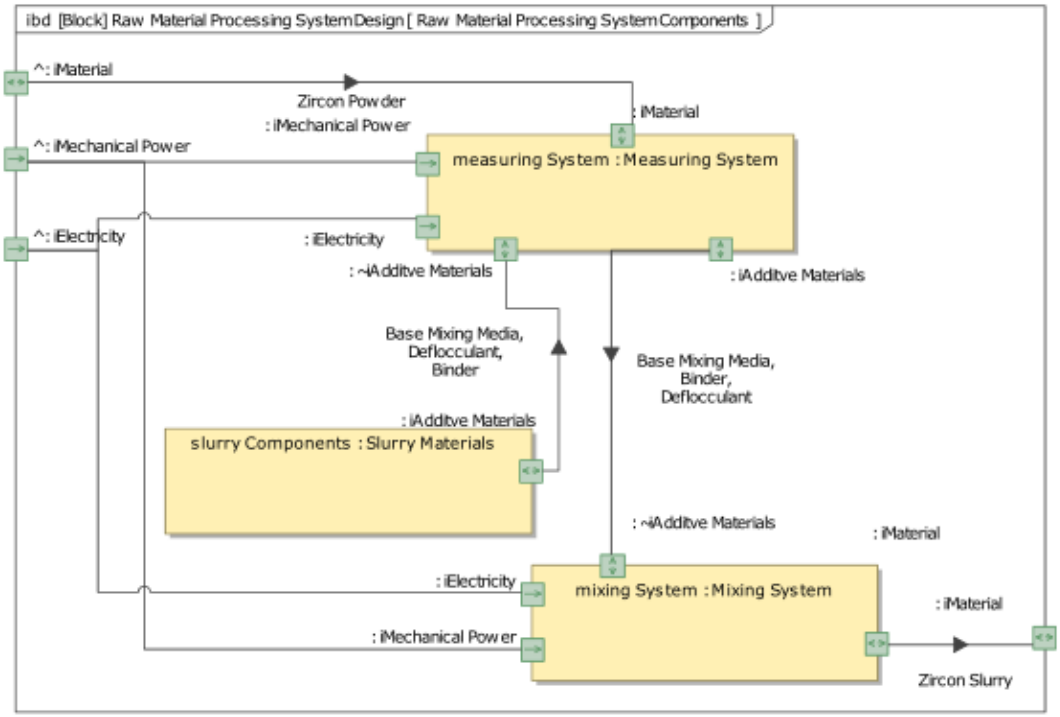

Figure 5.19: Logical Architecture of Raw Material Processing System

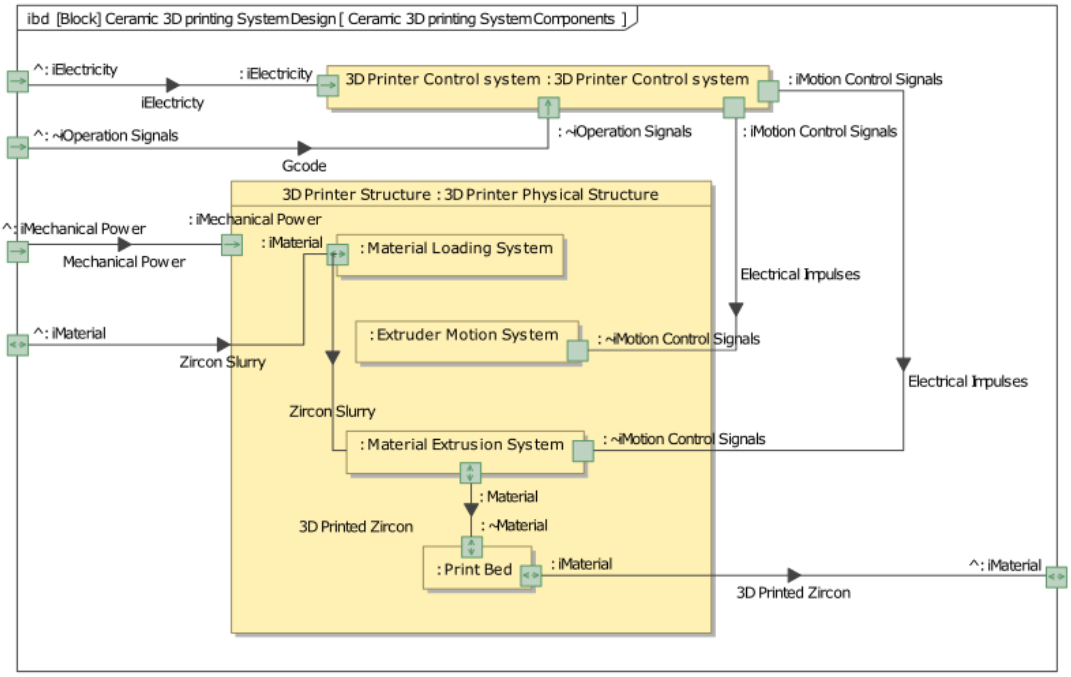

Figure 5.18: Logical Architecture of Ceramic 3D Printing System

Next, the behavior of each subsystem can be modeled. This is done using a combination of state machine diagram (stm) and activity diagram. The system behavior for the Control System is shown in Figure 5.20, in which a state machine diagram is followed by the activity diagrams that perform the desired function when the system is moving through that state. Once the subsystem structure modelling is complete, all the subsystems are integrated into the system of interest. The integrated system structure can be represented as a structure decomposition map shown in Figure 5.22. The most important aspect of the integration process is to make sure that the subsystem of the SIO are able to communicate with each other i.e. flow of material and information. This compatibility is shown in Figure 5.21, which represents the internal structure of the integrated SIO.

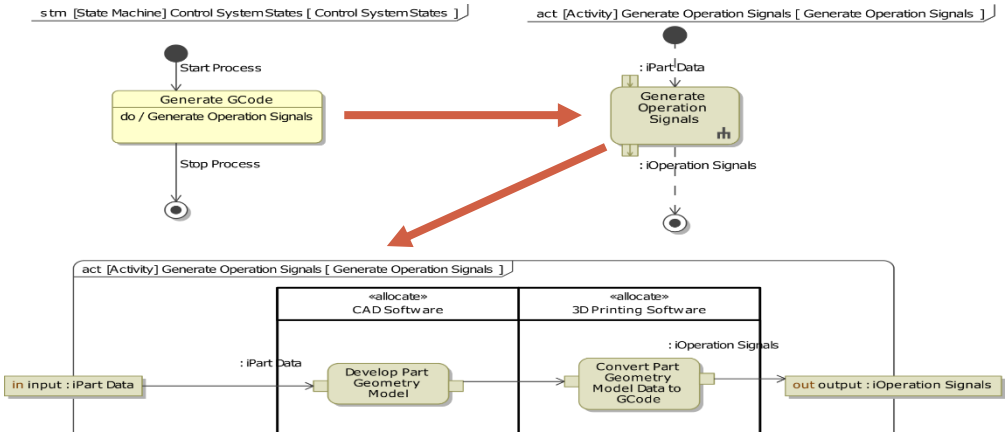

Figure 5.20: Control System – System Behavior (stm, activity)

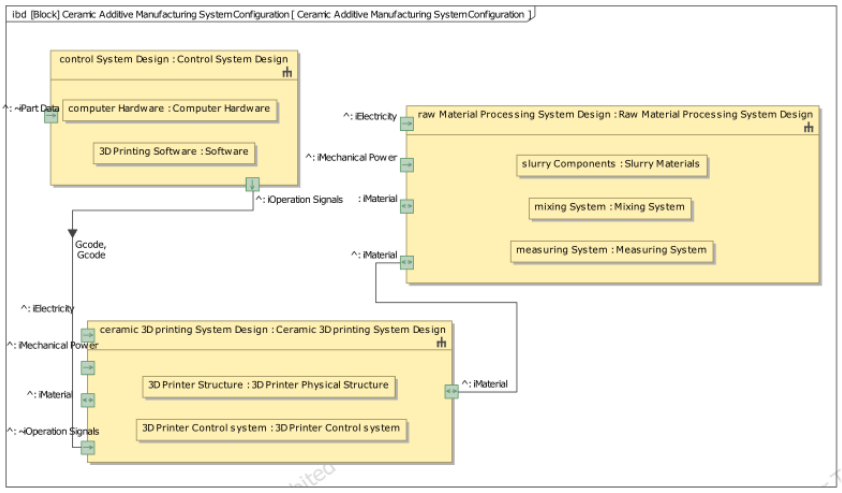

Figure 5.21: Ceramic Additive Manufacturing System Configuration

Figure 5.22: Structure Decomposition Map Ceramic Additive Manufacturing System

The final step to complete the modelling for the solution domain of the system, traceability is established between the different elements of the SIO and subsystems and the system requirement. Figure 5.23 shows a traceability matrix that captures the satisfy relationship between system requirements and the different elements of the system structure architecture. This process helps to validate that all the system requirements are satisfied and the system under design as a whole is capable to perform all the required functionalities captured through the stakeholder need analysis process.

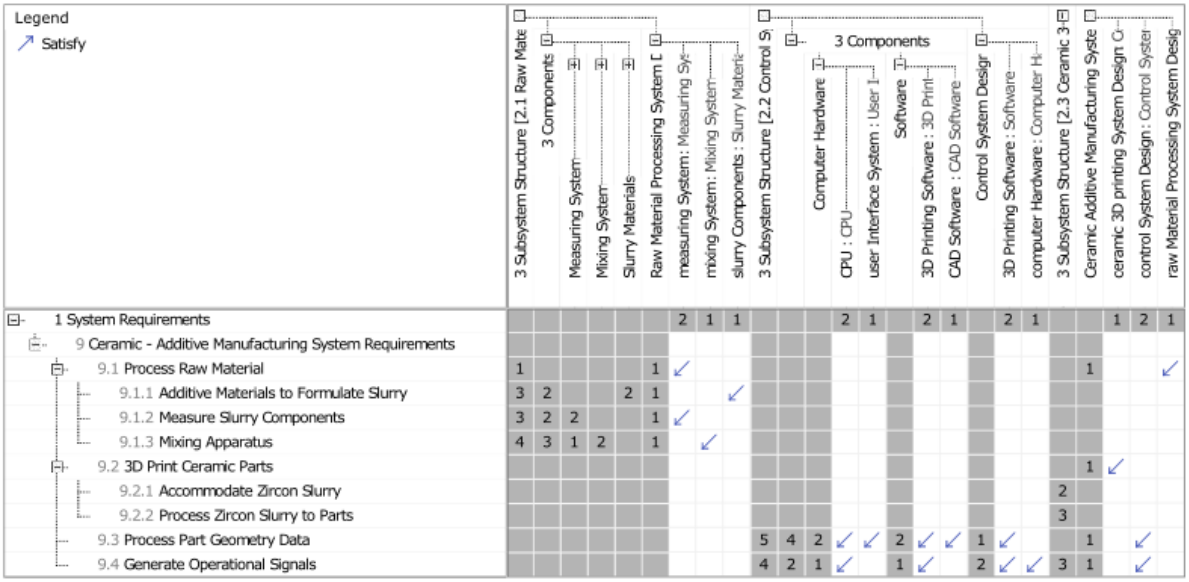

Figure 5.23: Traceability Matrix System Requirement – System Architecture

5.2.5 Implementation Domain Modeling

Implementation domain is the final stage in the system modelling process as per the MagicGrid framework. Once the Solution domain modelling is complete and the solution architecture of the SIO and subsystems is defined, the modelling of the implementation domain can begin. As per the MBSE process and the MagicGrid approach after the implementation domain the actual physical system and its subsystems are ready for detail engineering design. In this stage of the modelling, based on the defined solution architecture, the system requirements, functional analysis performed through the modelling of the problem and solution domain, detailed physical requirements of the SIO can be modeled. This done through the use of SysML requirements diagram. In this study the physical requirements for each subsystem i.e. Raw Material Processing

System, Control System and 3D Printer System are modelled separately as shown in Figure 5.24, Figure 5.25 and Figure 5.26 respectively. It is to be noted that as the different subsystem are developed separately, a set of detailed requirements with regards to specification is recommended to be developed. However in this study, since the system development of the actual ceramic additive manufacturing process was not carried out in parallel with the MBSE process the details regarding the exact specifications for example the specification of the actual Ball mill used for the slurry formulation process are not captured in the model.

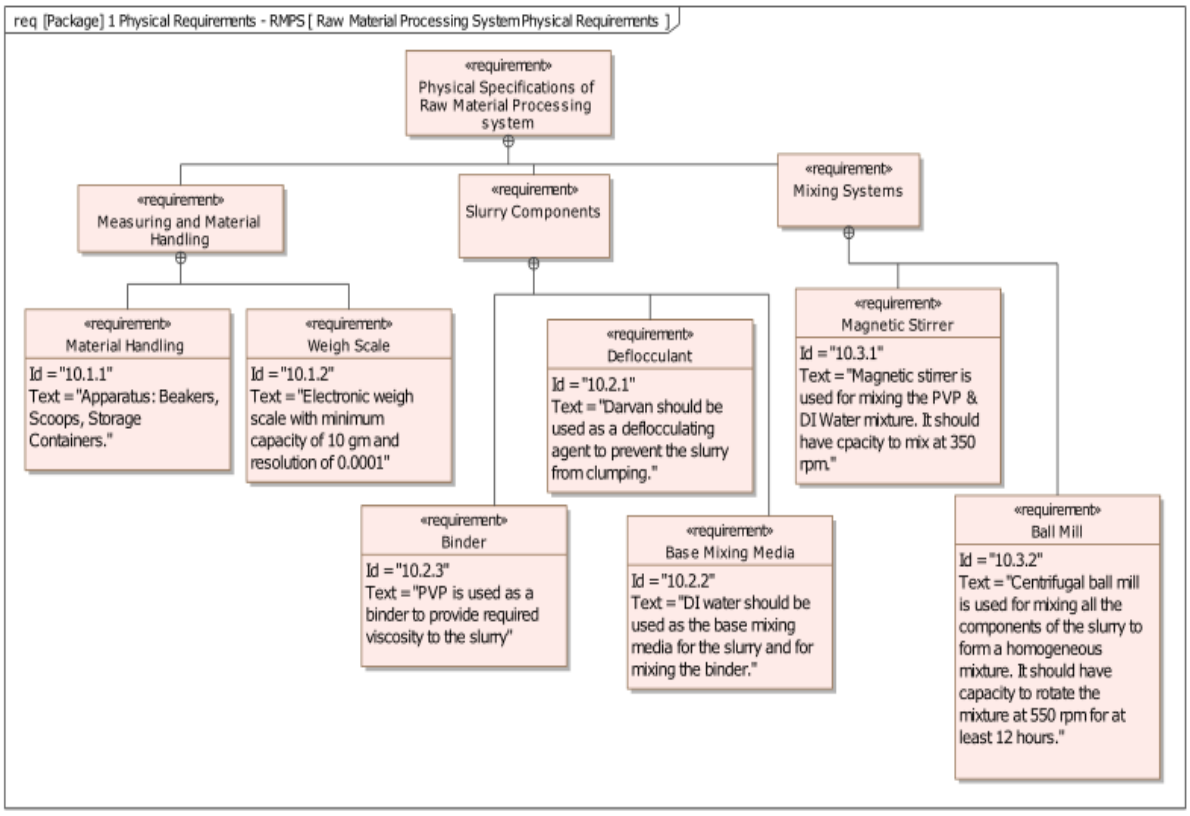

Figure 5.24: Raw Material Processing System – Physical Requirement

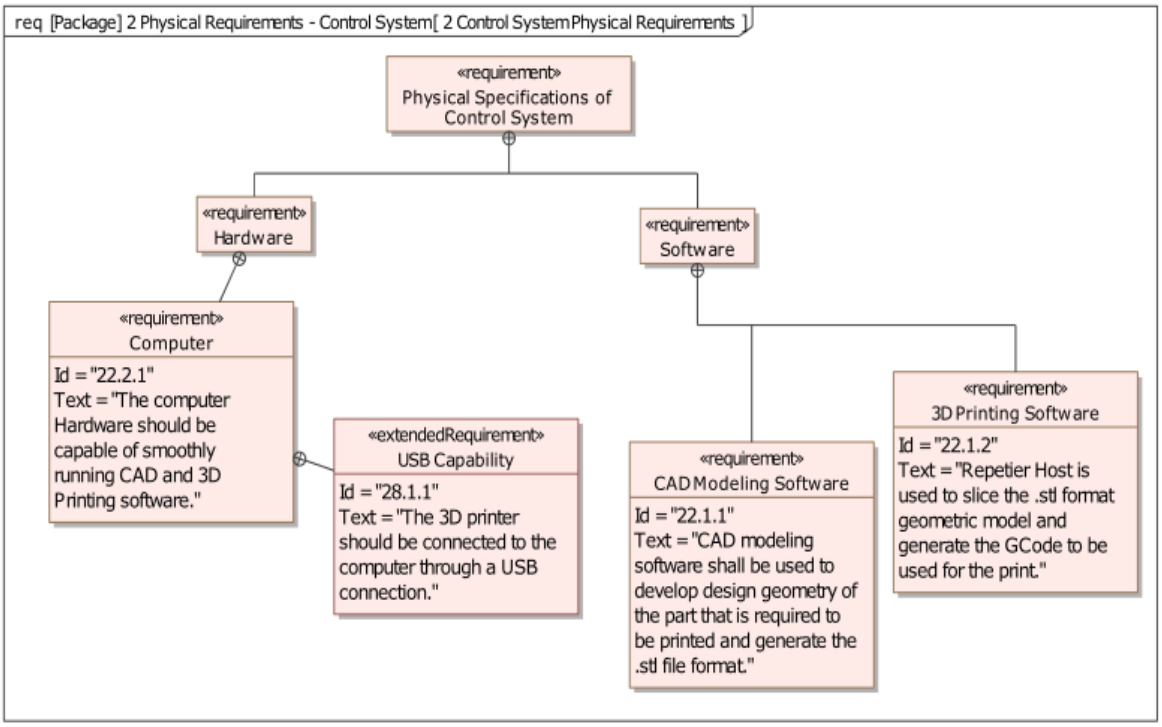

Figure 5.26: Control System – Physical Requirements

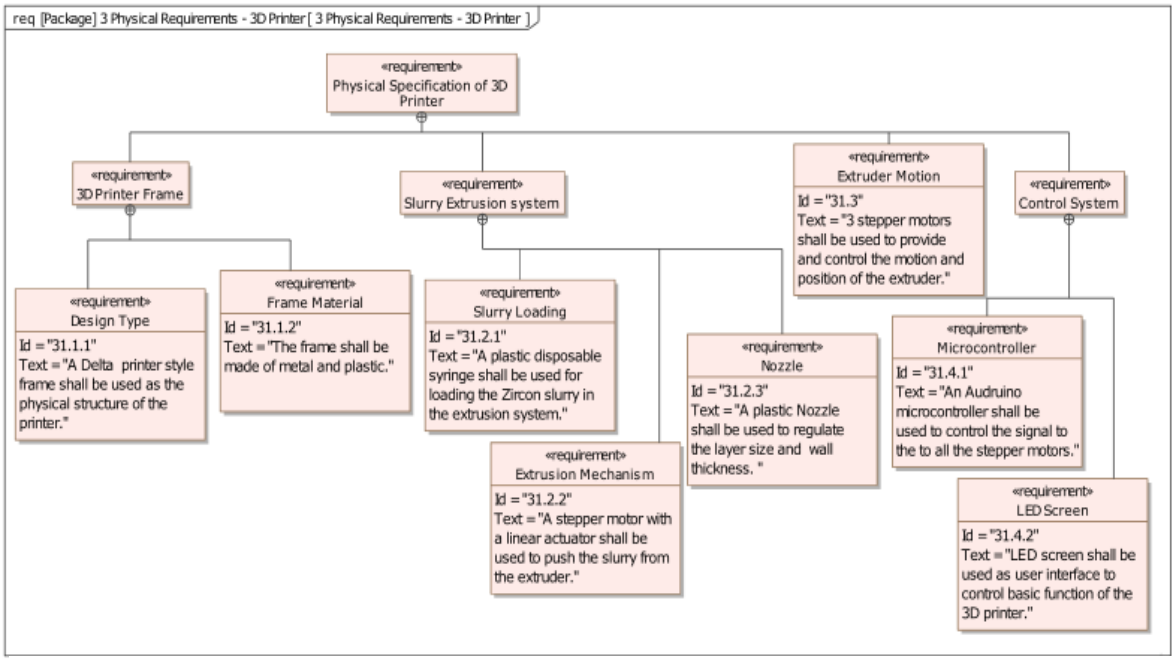

Figure 5.25: 3D Printer System – Physical Requirements

Once all the physical requirements of the SIO are captured and modelled, a downstream impact analysis with respect to the evolution of the model from a very abstract level requirement definition to the detailed physical requirements, a requirement decomposition map is used. This SysMl artifact help to understand the traceability between requirements at the implementation and solution domain level and the stakeholder needs at the problem domain level. Figure 5.27 shows the requirement decomposition map depicting which of the requirement have derived from a higher level of abstraction and which have been newly created through functional, operational, subsystem architecture analysis.

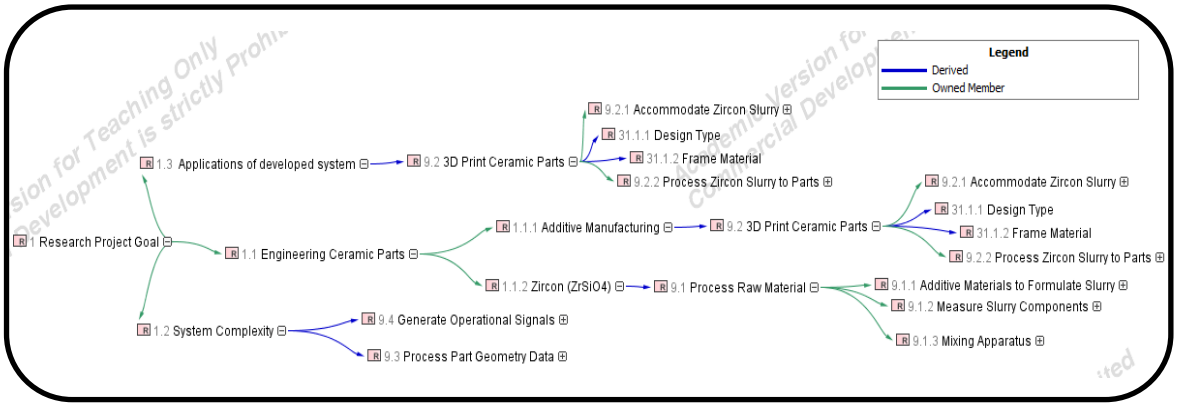

Figure 5.27: Requirement Decomposition Map for Ceramic Additive Manufacturing System

6. SUMMARY AND FUTURE WORK

6.1 Summary

In this work, we have developed a 3D printer system by modifying a filament based Delta printer and converting it to be capable of printing ceramic material in slurry form. This was done by incorporating a customized extrusion mechanism in which the ceramic slurry can be loaded and the required part geometry can be 3D printed. The major summary of the work is summarized as follows.

- A highly loaded aqueous slurry of Zircon is formulated by using DI water as the base mixing media, PVP as the binder, Darvan® 821A as the deffloculant agent and zircon powder
- Through experimentation, an ideal slurry composition was developed to formulate slurry with viscosity suitable for good quality printing. The ideal slurry composition in term of vol% is zircon 86.9vol%, PVP 1.6vol%, Darvan® 821A 1.04vol%, and DI water 10.4 vol%
- Through various print trails, it is observed that the nozzle diameter, the print bed temperature and the extrusion multiplier value are the printing parameters that had the most significant impact on the quality of the printed specimen. It is also observed that due to the inconsistent nature of the slurry these parameters required tweaking based on the slurry quality to obtain a good quality print
- Through formulation of good quality slurry and optimized printing parameters, zircon parts are successfully 3D printed. The printed parts included simple continuous geometry parts such a thin-walled high aspect ratio cylinder as well as complex geometry parts such as honeycomb structures
- Application of 3D printing technology towards production of molds using zircon is successfully demonstrated. Simple turbine shaped mold is 3D printed and solder metal is used as a demo material to cast a part using the printed mold. It is observed that the cast part develops surface imprints similar to the mold due to the inherent layered structure of the 3D printing process. Surface finishing process post casting is required to obtain smooth surface parts

- Zircon samples are heat-treated and material testing is done to study the effect of heat treatment on the slurry material. Through hardness testing it is observed that the hardness value of the samples initially increase with increase in temperature up to 225°C almost by 50% as compared to green-state part. However, beyond this temperature range, the hardness value decreases sharply due to the formation of micropores in the microstructure as the binder and the deflocculant are decomposed. Through SEM analysis, it is observed that the microstructure is the most dense at 225°C heat-treatment range with porosity increasing as the temperature increases as reflected in the behavior trend of the hardness testing results. Through the results of XRD analysis it is seen that there is no change in phase when the samples are heat-treaded due to the thermal stability of Zircon up to a temperature of 1673°C
- Ceramic Additive Manufacturing system is modeled using the MBSE principles and application of MagicGrid framework. Through the modelling process, the logical level functionalities of the system of interest are captured and a logical solution architecture is developed.
- Using MagicGrid framework, captured the system requirements, behaviors, functionalities, and physical architecture.

6.2 Future Work

Although the achievements made through this thesis work, the following items are identified to improve in the future.

- A more robust 3D printing system needs to be developed to utilize the capabilities of using extrusion based ceramic 3D printing to produce parts with complex and intricate geometries.
- Further studies need to be performed to understand the feasibility of using 3D printing to produce mold from zircon with respect to dimensional accuracy and surface finish issues and compatibility of the proposed process with practical casting materials.
- Further analysis in terms of material testing needs to be performed to understand the behavior of the slurry material when useable parts are 3D printed.
- More intensive system engineering effort needs to be utilized to capture the system to a much higher level of abstraction, to develop a system model robust enough to serve as a base for development of similar systems. Collaborative effort should be employed to capture the system requirements and behavior to a much greater detail so that multiple system solutions can be developed and trade-off studies can be performed to develop the most complete architecture for the system.

REFEENCES

[1] Z. Chen *et al.*, "3D printing of ceramics: A review," *J. Eur. Ceram. Soc.*, vol. 39, no. 4, pp. 661–687, 2019.

[2] G. Mitteramskogler *et al.*, "Light curing strategies for lithography-based additive manufacturing of customized ceramics," *Addit. Manuf.*, vol. 1, pp. 110–118, 2014.

[3] W. Chu *et al.*, "Centimeter-Height 3D Printing with Femtosecond Laser Two-Photon Polymerization," *Advanced Materials Technologies*, vol. 3, no. 5. 2018.

[4] R. He *et al.*, "Fabrication of complex-shaped zirconia ceramic parts via a DLP-stereolithography-based 3D printing method," *Ceram. Int.*, vol. 44, no. 3, pp. 3412–3416, 2018.

[5] N. Peretyagin, A. Seleznev, and P. Peretyagin, "Direct ink writing technology (3d printing) of graphene-based ceramic nanocomposites: A review," *Nanomaterials*, vol. 10, no. 7, pp. 1–48, 2020.

[6] P. E. P. Walsh, "United States Patent (19)," no. 19, 1994.

[7] I. Shishkovsky, I. Yadroitsev, P. Bertrand, and I. Smurov, "Alumina-zirconium ceramics synthesis by selective laser sintering/melting," *Appl. Surf. Sci.*, vol. 254, no. 4, pp. 966–970, 2007.

[8] C. Griffin, J. Daufenbach, and S. McMillin, "Solid Freeform Fabrication of Functional Ceramic Components Using a Laminated Object Manufacturing Technique," *Solid Free. Fabr. Conf.*, pp. 17–25, 1994.

[9] A. Ahmad, S. Darmoul, W. Ameen, M. H. Abidi, and A. M. Al-Ahmari, "Rapid prototyping for assembly training and validation," *IFAC-PapersOnLine*, vol. 28, no. 3, pp. 412–417, 2015.

[10] H. Elsner, "Assessment Manual: Heavy Minerals of Economic Importance," *Bgr*, p. 222, 2007.

[11] C. Range, "Strategic Minerals Inventory Summary Report - Zirconium," 1987.

[12] M. Lines, "An overview of the mineral sands industry," *AusIMM Bull.*, no. 2, pp. 38–41, 2008.

[13] A. Kaiser, M. Lobert, and R. Telle, “Thermal stability of zircon (ZrSiO4),” *J. Eur. Ceram. Soc.*, vol. 28, no. 11, pp. 2199–2211, 2008.

[14] M. R. Anseau, C. Leblud, and F. Cambier, “Reaction sintering (RS) of mixed zircon-based powders as a route for producing ceramics containing zirconia with enhanced mechanical properties,” *J. Mater. Sci. Lett.*, vol. 2, no. 7, pp. 366–370, 1983.

[15] D. Owen *et al.*, “3D printing of ceramic components using a customized 3D ceramic printer,” *Prog. Addit. Manuf.*, vol. 3, no. 1, pp. 3–9, 2018.

[16] S. Dhara, R. K. Kamboj, M. Pradhan, and P. Bhargava, “Shape forming of ceramics via gelcasting of aqueous particulate slurries,” *Bull. Mater. Sci.*, vol. 25, no. 6, pp. 565–568, 2002.

[17] J. H. Song and J. R. G. Evans, “Flocculation after injection molding in ceramic suspensions,” *J. Mater. Res.*, vol. 9, no. 9, pp. 2386–2397, 1994.

[18] R. T. V. Company, “Technical Data - DARVAN® 821-A Ammonium Dispersing Agent for Ceramic Bodies,” p. 821, 2014.

[19] M. A. Janney, O. O. Omatete, C. A. Walls, S. D. Nunn, R. J. Ogle, and G. Westmoreland, “Development of low-toxicity gelcasting systems,” *J. Am. Ceram. Soc.*, vol. 81, no. 3, pp. 581–591, 1998.

[20] V. L. Wiesner, “Fabricating Complex-Shaped Components by Room-Temperature Injection Molding of Aqueous Ceramic Suspension Gels,” vol. 9, pp. 1–157, 2013.

[21] V. L. Wiesner, J. P. Youngblood, and R. W. Trice, “Room-temperature injection molding of aqueous alumina-polyvinylpyrrolidone suspensions,” *J. Eur. Ceram. Soc.*, vol. 34, no. 2, pp. 453–463, 2014.

[22] L. Rueschhoff, W. Costakis, M. Michie, J. Youngblood, and R. Trice, “Additive Manufacturing of Dense Ceramic Parts via Direct Ink Writing of Aqueous Alumina Suspensions,” *Int. J. Appl. Ceram. Technol.*, vol. 13, no. 5, pp. 821–830, 2016.

[23] K. Mohanta and P. Bhargava, “Effect of milling time on the rheology of highly loaded aqueous-fused silica slurry,” *Journal of the American Ceramic Society*, vol. 91, no. 2. pp. 640–643, 2008.

[24] S. Tang, L. Yang, G. Li, X. Liu, and Z. Fan, “3D printing of highly-loaded slurries via layered extrusion forming: Parameters optimization and control,” *Addit. Manuf.*, vol. 28, no. June, pp. 546–553, 2019.

[25] F. Nakamori, Y. Ohishi, H. Muta, K. Kurosaki, K. ichi Fukumoto, and S. Yamanaka, "Mechanical and thermal properties of ZrSiO4," *J. Nucl. Sci. Technol.*, vol. 54, no. 11, pp. 1267–1273, 2017.

[26] BKCASE Editorial Board, "Guide to the Systems Engineering Body of Knowledge," *Guid. to Syst. Eng. Body Knowl.*, no. May, p. 945, 2016.

[27] International Council on Systems Engineering (INCOSE), "Systems Engineering Vision 2020," *Syst. Eng. Vis. 2020*, no. September, p. 32, 2007.

[28] K. Kalvit, "Application of an innovative MBSE (SysML-1D) co-simulation in healthcare." 2018.

[29] C. Wylie, "'Book of knowledge.,'" *Notes Queries*, vol. s2-II, no. 31, p. 90, 1856.

[30] A. Morkevicius, A. Aleksandraviciene, D. Mazeika, L. Bisikirskiene, and Z. Strolia, "MBSE Grid: A Simplified SysML-Based Approach for Modeling Complex Systems," *INCOSE Int. Symp.*, vol. 27, no. 1, pp. 136–150, 2017.

PUBLICATIONS

- **3D Printing of Biomimetically Inspired Zircon for Ceramic Mold Components**, P.P. Raikar, T.C. Dube, A. Tiamiyu, A.D. Ekwealor, A.S. Panuganti, C.C. Shorey, H.Y. Park, J. Zhang, Y.G. Jung POWDERMET/AMPM 2019, Phoenix, AZ , USA; June 2019
- **Optimization of Printing Parameters for 3D Printed PLA**, N.H. Hawaldar, P.P. Raikar, T.C. Dube, J. Zhang MS&T Conference, Columbus, OH, USA; October 2018
- **3D printing of ceramic components using a customized 3D ceramic printer**, D.Owen, J.Hickey, A. Cusson, O.I. Ayeni, J. Rhoades, Y. Deng, Y. Zhang, L.Wu, H.Y. Park, N.H. Hawaldar, P.P. Raikar, Y.G. Jung, J. Zhang Progress in Additive Manufacturing, vol. 3,no. 1, pp 3-9,2018

.